The definition of reaction coordinates for reaction-path dynamics

Gregory A. Natanson
Computer Sciences Corporation, Seabrook, Maryland 20706

Bruce C. Garrett
Molecular Science Research Center, Pacific Northwest Laboratory, Richland, Washington 99352

Thanh N. Truong, Tomi Joseph, and Donald G. Truhlar
Department of Chemistry and Supercomputer Institute, University of Minnesota, Minneapolis, Minnesota 55455-0431

We present equations for generalized-normal-mode vibrational frequencies in reaction-path calculations based on various sets of coordinates for describing the internal motions of the system in the vicinity of a reaction path. We consider two special cases in detail as examples, in particular three-dimensional atom–diatom collisions with collinear steepest descent paths and reactions of the form $CX_3 + YZ \rightarrow CX_3 Y + Z$ with reaction paths having C_{3v} symmetry. We then present numerical comparisons of the differences in harmonic reaction-path frequencies for various coordinate choices for three such systems, namely, $H + H_2 \rightarrow H_2 + H$, $O + H_2 \rightarrow OH + H$, and $CH_3 + H_2 \rightarrow CH_4 + H$. We test the importance of the differences in the harmonic frequencies for dynamics calculations by using them to compute thermal rate constants using variational transition state theory with semiclassical ground-state tunneling corrections. We present a new coordinate system for the reaction $CH_3 + H_2$ that should allow for more accurate calculations than the Cartesian system used for previous reaction-path calculations on this and other polyatomic systems.

I. INTRODUCTION

In many cases, the atoms involved in typical chemical reactions explore only small-amplitude deviations from a minimum-energy path (MEP) through nuclear coordinate space. Thus, many workers have attempted to treat such reactions by using an explicit reaction path.[1-34] However, the choice of coordinate system is very important for making such calculations practical and accurate.

In choosing the coordinate system, the critical issue is the definition of the reaction coordinate. Along the reaction path, the reaction coordinate s is uniquely defined as the negative or positive distance from the point on the reaction path to the saddle point configuration. For geometries off the reaction path, definition of the reaction coordinate requires mapping the geometry onto the reaction path and this mapping is not unique. As a simple example, consider the definition of the reaction coordinate for the collinear reaction $A + BC \rightarrow AB + C$. Figure 1 displays a schematic of potential energy contours for the reaction in mass-scaled coordinates; in particular,[18] x is the distance of A from the center-of-mass of BC and y is the BC distance scaled to the same reduced mass as the x motion. The conventional definition of the reaction coordinate for a geometry x_0, y_0 not on the reaction path is to map x_0, y_0 onto the closest point on the reaction path (the straight line in Fig. 1). An alternative choice is to map x, y onto the reaction path along arcs which intersect the reaction path at right angles. Although questions arise as to whether the latter choice of reaction coordinate may provide a practical or accurate computational scheme, this does illustrate that a geometry off the reaction path can be mapped onto two distinct values of the reaction coordinate s.

Two particular choices of reaction coordinate that are both based on the minimum-energy path (MEP) through mass-scaled coordinates have been widely applied to atom–diatom reactions in which the MEP is collinear. In both cases the reaction coordinate for arbitrary collinear geometries is defined by the conventional prescription outlined above—mapping the geometry onto the closest point on the reaction path. However, for bent geometries the two definitions differ. In one choice the value of the reaction coordi-
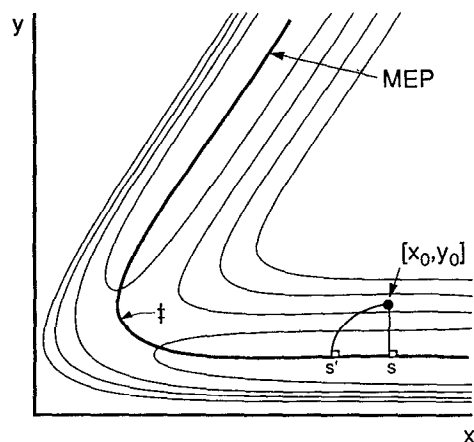

FIG. 1. Illustration of a possible ambiguity in defining the reaction coordinate for geometries not on the minimum energy path (MEP). Potential energy contours are displayed in mass scaled and skewed coordinates (see text). The heavy line is the minimum energy path. Two possible mappings of the geometry (x_0, y_0) are displayed: a straight line segment connecting the geometry with location s on the MEP and an arc connecting the geometry with the location s' on the MEP.

nate is fixed when the triatomic is bent with constant AB and BC bond distances [Fig. 2(a)]. In the other choice s is fixed when the triatomic is bent along generalized normal modes consisting of linear combinations of mass-scaled Cartesian displacements from the reaction path [Fig. 2(b)]. The goal of the present paper is to compare these choices of coordinate systems in detail and to show by example how to extend the former to a more general class of reactions involving more than three atoms.

We will place particular emphasis on the harmonic approximation for small-amplitude vibrations in the vicinity of the MEP. The harmonic approximation for small-amplitude vibrations in the vicinity of a potential minimum is of course well known in infrared spectroscopy. In that case one begins with either internal coordinates or Cartesian coordinates, truncates the expansion of the potential at quadratic terms, and transforms to a set of normal coordinates that are uncoupled in the kinetic energy and simultaneously—through quadratic terms—in the potential energy. The uncoupled coordinates are the normal modes, and they are associated with a unique set of frequencies. Although the initial coordinate choice does not affect these frequencies, it is very significant for treating higher-order terms in the potential energy, for large-amplitude vibrations, and for vibration–rotation coupling.

We will demonstrate in the present paper that the harmonic approximation to the local vibrational motion on the MEP has a significantly greater dependence on the coordinate choice at a nonstationary point than a stationary one; in particular, even the harmonic frequencies are coordinate dependent as a consequence of the fact that the gradient does not vanish at the origin of the expansion.[23]

In Sec. II we present a general mathematical framework for defining reaction-path coordinate systems and for calculating the dependence of harmonic reaction-path frequencies on coordinate choice. In Sec. III we explicitly compare the Cartesian and bond-length–bond-angle choices for atom–diatom reactions in this framework, and we extend the latter choice to reactions of the form

$$CH_3 + XY \rightarrow CH_3X + Y,$$
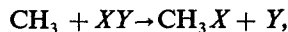
where the reaction path has C_{3v} symmetry. In Sec. IV we present illustrative applications for the reactions
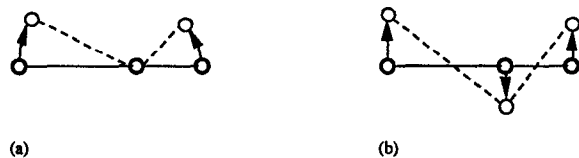

(a)   (b)

FIG. 2. Bending motions along a curvilinear bend coordinate corresponding to constant AB and BC bond lengths and also along a generalized normal mode. Part (a) shows the mapping of a bent geometry onto a collinear geometry in which the bond lengths are kept constant. Part (b) depicts the mapping of a bent geometry to the collinear MEP along straight-line Cartesian displacements.

$$H + H_2 \rightarrow H_2 + H, \tag{R1}$$

$$O + H_2 \rightarrow OH + H, \tag{R2}$$

and

$$CH_3 + H_2 \rightarrow CH_4 + H \tag{R3}$$

and we compare the numerical results for the harmonic frequencies. We also test the importance of the different choice of reaction coordinate on calculations of thermal rates within a reaction-path framework using variational transition state theory with semiclassical adiabatic tunneling corrections. Finally, a discussion, summary, and conclusions are presented in Sec. V.

II. THEORY

We begin by defining the MEP in mass-scaled coordinates. The mass-scaled coordinates are defined by

$$r_1 = (m_A/\mu)^{1/2} x_A, \tag{1a}$$

$$r_2 = (m_A/\mu)^{1/2} y_A, \tag{1b}$$

$$\cdots$$

$$r_{3N} = (m_N/\mu)^{1/2} z_N, \tag{1c}$$

where m_A, m_B,...,m_N are atomic masses, x_A, y_A, and z_A are Cartesian coordinates of atom A, and μ is an arbitrary mass, which will be called the reduced mass. Then the MEP is defined as the path of steepest descents through the mass-scaled coordinate system starting at a saddle point. If $\mathbf{r} = \mathbf{a}(s)$ at point s on the MEP, and $\mathbf{r} = \mathbf{r}^{\neq}$ at the saddle point—which will be taken as the origin of the MEP, i.e., $s = 0$—then the MEP satisfies

$$\frac{d\mathbf{a}}{ds} = +\mathbf{v}, \tag{2}$$

with initial conditions

$$\mathbf{a}(0) = \mathbf{r}^{\neq}, \tag{3}$$

where

$$\mathbf{v} = -\nabla_r V/|\nabla_r V| \tag{4}$$

and V is the potential energy. The coordinate s is defined on the MEP as the signed distance along the MEP. In addition to s, the potential energy depends on $3N-7$ other internal coordinates. (By definition, any internal coordinate remains unchanged when the molecular system rotates as a whole.) The other internal coordinates, excluding s, are denoted q_1, q_2,...,q_{F-1}, and they vanish by definition along the reaction path. In addition, we define $q_F = s$; and we let $\mathbf{q} = (q_1, q_2,...,q_F)$ denote the complete set of internal coordinates. We denote the momenta conjugate to $\mathbf{q}$ as $\mathbf{p}$. Any derivative of the form $\partial f/\partial q_i$ should be interpreted as requiring $q_1,...,q_{i-1}$, $q_{i+1},...,q_F$ be held fixed. This includes $\partial f/\partial s$, which should be interpreted technically as $\partial f/\partial q_F$. We neglect vibration–rotation coupling and thus all further analysis is done without reference to overall rotations and translations. In internal coordinates the nonrotating classical system is governed by the Hamiltonian:

$$H = \frac{1}{2} \sum_{i,j}^{F} G_{ij}(\mathbf{q}) p_i p_j + V(\mathbf{q}), \tag{5}$$

where the coefficient of momentum coupling for an arbitrary internal coordinate system is[35]

$$G_{ij} = \frac{1}{\mu} (\nabla_r q_i) \cdot (\nabla_r q_j). \tag{6}$$

It is particularly convenient if the coordinates **q** are defined such that three conditions hold:

(i) All coefficients G_{ij} of cross terms $p_i p_j$, $i \neq j$, should vanish on the MEP.

(ii) The only linear term in the expansion of the potential energy in a Taylor series at a point s_0 on the MEP should be proportional to $(s-s_0)$. This requires

$$\left(\frac{\partial V}{\partial q_i} \right)\Big|_{r=a(s)} = 0, \quad i = 1,2,...,F-1. \tag{7}$$

This is clearly equivalent to

$$\left(\frac{\partial r}{\partial q_i} \right)\Big|_{r=a(s)} \cdot \frac{\partial V}{\partial r} = 0 \tag{8}$$

and, hence, by Eqs. (2) and (4), to

$$\left(\frac{\partial r}{\partial q_i} \right)\Big|_{r=a(s)} \cdot \frac{\partial a}{\partial s} = 0; \tag{9}$$

in other words, the vibrational coordinates should be locally orthogonal to the MEP.

(iii) The quadratic potential coupling of the reaction coordinate to the vibrational coordinates should vanish, i.e.,

$$\frac{\partial^2 V}{\partial q_i \partial s} = 0, \quad i = 1,...,F-1. \tag{10}$$

This is easily proved by differentiating Eq. (7) with respect to s. As a consequence, the Wilson **G** and **F** matrices[35] both decouple into an $(F-1) \times (F-1)$ vibrational submatrix and a 1×1 reaction path element.

Next we consider the vibrational submatrix of **F**, i.e.,

$$F_{ij}(s_0) = \left(\frac{\partial^2 V}{\partial q_i \partial q_j} \right)_{s_0}, \tag{11}$$

where $q_1,...,q_{i-1}, q_{i+1},...,q_F$ are held fixed in any derivative $\partial f / \partial q_i$, and the subscript in Eq. (11) means that s is held fixed at the value s_0. The potential in the vicinity of a point s_0 on the MEP may be written

$$V(q_1,...,q_{F-1},s_0) = V_{MEP}(s_0) + \frac{1}{2} \sum_{i=1}^{F-1} \sum_{j=1}^{F-1} F_{ij}(s_0)q_i q_j. \tag{12}$$

First we note that, to assign natural collision coordinates to a point off the MEP, we *first* assign s, *then* the vibrational coordinates. For a given definition of s, including the definition of s off the MEP, the frequencies are independent of the choice of the vibrational coordinates, as long as the latter are orthogonal to the MEP at $\mathbf{q} = (0,...,0,s_0)$.[23] (The GF matrix undergoes a similarity transformation when it is transformed from one set of vibrational coordinates to another provided that the reaction coordinate s is kept unchanged.) However, the frequencies do depend on the definition of s for points off the MEP. For example, given a global definition of s, suppose we change it in the vicinity of the MEP as follows:

$$s' = s + \sum_{i}^{F-1} \sum_{j}^{F-1} b_{ij}(s)q_i q_j + 0(q_i^3). \tag{13}$$

We note that the linear term is missing in Eq. (13) because the first derivatives of s and s' with respect to **r** coincide at $\mathbf{q} = (0,...,0,s)$ and we also note that the b matrix is symmetric because of the symmetry of mixed second derivatives. Since the only nonzero first derivative of the potential on the MEP is that with respect to s one finds[23]

$$\left(\frac{\partial^2 V}{\partial q_i \partial q_j} \right)_{s'}\Big|_{\mathbf{q}=(0,...,0,s')}$$
$$= \left[\left(\frac{\partial^2 V}{\partial q_i \partial q_j} \right)_s - b_{ij}\left(\frac{\partial V}{\partial s}\right)_{\mathbf{q}} \right]\Big|_{\mathbf{q}=(0,...,0,s)},$$
$$i,j = 1,2,...,F-1. \tag{14}$$

Except at stationary points of the potential, the **F** matrix defined by Eq. (11) can therefore be significantly altered by changes to the functions $b_{ij}(s) = b_{ji}(s)$. The calculation of harmonic frequencies requires diagonalization of the $(F-1) \times (F-1)$ submatrix of the **GF** matrix in the vibrational space where **G** is obtained by evaluating Eq. (6) on the MEP. At stationary points, the second term of Eq. (14) vanishes and thus the frequencies are invariant to the choice of coordinate system.

In practice, there are additional complications. One is that the effect of anharmonicity depends on the coordinate system, and the coordinate systems that are most convenient for separating vibrational motions from rotations may not lead to particularly accurate representations of the potential when truncated at quadratic (i.e., harmonic) terms. Thus, one may wish to consider vibrational coordinates for which the separation of internal motions from rotations is more difficult or only approximate. When we wish to refer to vibrational coordinates that are invariant under rotations, we will call them internal coordinates; when we refer to vibrational coordinates without this qualifier, we will include the possibility that they may be only approximately separable from rotation. In the following sections, we explore some practical treatments involving such coordinates.

III. HARMONIC FREQUENCIES FOR VARIOUS COORDINATE CHOICES

III A. Atom–diatom reactions with a collinear MEP

First we consider two coordinate systems for atom–diatom reactions $(A + BC \rightarrow AB + C)$ with a collinear MEP. In both cases, we use the same definition of the reaction coordinate s and the transverse stretch coordinate q_1 for all ABC collinear geometries. For bent geometries, however, the two definitions of s differ. In the first definition, s is fixed when the system is bent with constant A–B and B–C bond lengths.[3,20] This is called the bond-length reaction coordinate s^{BL}. In the second definition, s is fixed when the system is bent along a Cartesian generalized normal mode.[21] (Note: coordinates defined as a linear combination of Cartesians or mass-scaled Cartesians are also called Cartesian.) This is called the Cartesian-vibration reaction coordinate, s^{CV}. The two types of bending motion are illustrated in Fig. 2. To

define the Cartesian coordinates, linear configurations are placed along the z axis.

In previous calculations two sets of definitions of the doubly degenerate bending coordinates q_{2a} and q_{2b} have been used. First, a pair of bending angles measured in the yz and xz planes of a rotating frame have been used.[3,20] Second, the Cartesian generalized normal modes have been used.[21] The bending angles are examples of *curvilinear* vibrational coordinates since they *cannot* be written as linear combinations of Cartesians.

Because the bond-length and Cartesian-vibration reaction coordinates, s^{BL} and s^{CV}, are chosen to coincide for linear A–B–C configurations lying along the z axis, they lead to the same stretching frequency. However, the fact that they differ for nonlinear geometries manifests itself in a noticeable difference in bending harmonic frequencies—the subject of our present discussion. The difference between the harmonic frequencies comes from the necessity to evaluate second derivatives of the potential with different variables fixed. For example, in the bond-length reaction-coordinate system the AB and BC bond lengths are fixed, whereas in the Cartesian-vibration system, the derivatives are taken subject to the constraint of a fixed s^{CV}. Below we compare analytic expressions for the bending harmonic frequency evaluated along the same reaction path but using three different reaction-coordinate systems. The first two are prescriptions previously found in the literature, namely, (i) the intrabond angle combined with the bond-length reaction coordinate[3,20] and (ii) the coordinate system equivalent to the Miller–Handy–Adams description,[21] which is equivalent to using the Cartesian-vibration reaction coordinate combined with the Cartesian bending coordinate. Another reaction coordinate, defined via the Eckart–Sayvetz conditions[36,37] and referred to as the least-squares reaction coordinate s^{LS},[23] has some similarities with the Cartesian-vibration reaction coordinate and is utilized in Sec. III A 3 in combination with the intrabond angle. We will explicitly demonstrate the difference between the harmonic bending frequencies evaluated by means of the first two sets of variables and we will show that the latter two choices (i.e., those Secs. III A 2 and III A 3) give the same frequency (in agreement with the results of Ref. 23 that the harmonic frequencies evaluated at fixed values of the least-squares reaction coordinate with any choice of vibrational coordinates coincide with those calculated using the Miller–Handy–Adams projection technique).

III A 1. Bond-length reaction coordinate and intrabond angle

We start by evaluating the bending harmonic frequency by means of the bond-length reaction coordinate. This coordinate, s^{BL}, is a function of bond lengths only. It is defined on the MEP as the signed distance along the path with $s = 0$ at the saddle point. Then s is fixed when the system is bent with fixed bond lengths. [For a complete mathematical definition, one may use the bond-length scattering coordinates given in Eq. (22) of Ref. 38 and the relationships given by Marcus in Eq. (7) of Ref. 5]. We describe bending vibra-

tions by the deviation $\delta \equiv \pi - \Phi$ from linearity, where Φ is the angle between the A–B and B–C bonds, and we use the second derivative of the potential with respect to δ or, equivalently, with respect to Φ *at fixed values of the bond lengths.* We thus find[35]

$$[\omega_b^{BL}(s)]^2 = G_{\Phi\Phi}(s)F_{\Phi\Phi}(s), \tag{15}$$

where

$$G_{\Phi\Phi}^{-1}(s) = (\tilde{m}^2/I_0)(R_{BA}^2 R_{BC}^2)|_{r=a(s)}, \tag{16a}$$

$$F_{\Phi\Phi}(s) \equiv \left(\frac{\partial^2 V}{\partial\Phi^2}\right)_{R_{BA},R_{BC}}\Bigg|_{r=a(s)}, \tag{16b}$$

$$\tilde{m} \equiv (m_A m_B m_C/M)^{1/2}. \tag{17}$$

R_{BA}, R_{BC}, and R_{CA} are the AB, BC, and CA internuclear distances, M is the total nuclear mass, and I_0 is the largest principal moment of inertia evaluated along the MEP.

$$I_0 = (m_A m_B R_{BA}^2 + m_B m_C R_{BC}^2 + m_A m_C R_{CA}^2)/M|_{r=a(s)}. \tag{18}$$

In Eq. (16b) we use the fact that s^{BL} is a function only of the bond lengths so that holding s^{BL} fixed is equivalent to holding R_{BA} and R_{BC} fixed. As all the reaction coordinates considered in this paper coincide at each point along the MEP, we denote them simply as s there. Note that the harmonic bending frequency evaluated as above along the *collinear* reaction path coincides with that used in earlier work by two of the authors[20] who treated bending vibrations as a doubly degenerate normal mode (which is a superposition of bending motion and overall rotation). If the bending motion is treated as a *centrifugal* oscillator,[34,39] one obtains the same harmonic spectrum. [Alternatively, we can use Eqs. (16a), (17), and (18) to write

$$[\omega_b^{BL}(s)]^2 = \left[\frac{1}{m_A R_{BA}^2} + \frac{1}{m_C R_{BC}^2} + \frac{1}{m_B}\right. $$
$$\left. \times\left(\frac{R_{CA}}{R_{BA}R_{BC}}\right)^2\right]F_{\Phi\Phi}(s), \tag{19}$$

which is clearly equivalent to the version we have used previously[20] for collinear MEPs.]

For comparison with other choices of reaction coordinate, it is convenient to assume that the potential V is a well defined function of the three interatomic distances R_{BA}, R_{BC}, and R_{CA}. Derivatives of the potential with respect to the nuclear Cartesian coordinates r_d are obtained from derivatives with respect to the interatomic distances by the chain rule. The resulting expressions are rigorously correct even for linear configurations where the interatomic distances become redundant. The use of the interatomic distances as an intermediate set of internal variables makes it possible to represent the second derivatives of the potential with respect to the Cartesian coordinates in a very compact form as shown below in Sec. III A 2. To facilitate relating the final expressions for the bending frequencies evaluated in

different sets of coordinates, the second derivatives on the right side of Eq. (16b) are given in terms of the first derivative of the potential with respect to R_{CA} at fixed values of the bond lengths R_{BA} and R_{BC} by the following expressions

$$\left(\frac{\partial^2 V}{\partial \Phi^2}\right)_{R_{BA},R_{BC}} = \left(\frac{\partial^2 V}{\partial R_{CA}^2}\right)_{R_{BA},R_{BC}} \left(\frac{\partial R_{CA}}{\partial \Phi}\right)^2_{R_{BA},R_{BC}}$$
$$+ \left(\frac{\partial V}{\partial R_{CA}}\right)_{R_{BA},R_{BC}} \left(\frac{\partial^2 R_{CA}}{\partial \Phi^2}\right)_{R_{BA},R_{BC}},$$
$$(20)$$

where the CA bond length is related to the bending angle by

$$R_{CA}^2 = R_{BA}^2 + R_{BC}^2 - 2R_{BA}R_{BC} \cos \Phi. \qquad (21)$$

The first derivative of R_{AC} with respect to Φ vanishes in any linear configuration so that

$$F_{\Phi\Phi}|_{\Phi = \pi} = \left[\left(\frac{\partial V}{\partial R_{CA}}\right)_{R_{BA},R_{BC}} \left(\frac{\partial^2 R_{CA}}{\partial \Phi^2}\right)\right]\bigg|_{\Phi = \pi}$$
$$= -\frac{R_{BA}R_{BC}}{R_{CA}} \left(\frac{\partial V}{\partial R_{CA}}\right)_{R_{BA},R_{BC}}\bigg|_{\Phi = \pi} \qquad (22)$$

and hence

$$[\omega_b^{BL}(s)^2] = -\frac{I_0}{\tilde{m}^2}\left[\frac{1}{R_{BA}R_{BC}R_{CA}}\right.$$
$$\left. \times\left(\frac{\partial V}{\partial R_{CA}}\right)_{R_{BA},R_{BC}}\right]\bigg|_{r = a(s)}. \qquad (23)$$

We immediately conclude that the right side of Eq. (23) is positive whenever the interaction between atom A and C is pairwise repulsive. Therefore, simple potential models with end-atom pair repulsions, such as the BEBO[3] and RMBEBO[20(a)] models, will always give real bending frequencies in the bond-length coordinates.

III A 2. Cartesian-vibration reaction coordinate and Cartesian bending coordinate

The bending frequency in the Cartesian-vibration reaction coordinate system can be obtained most conveniently by the prescription of Miller, Handy, and Adams.[21] The frequencies for the vibrational modes orthogonal to the reaction coordinate are found by first projecting out infinitesimal rotations and center-of-mass translations before diagonalizing the mass-weighted Hessian matrix. For the triatomic reaction with collinear MEP, the problem is greatly simplified because the Hessian matrix and projection matrix can be put into block diagonal form with three 3×3 submatrices. To do this, we choose our Cartesian system so that for collinear geometries along the MEP the atoms are constrained to lie along the z axis with $z_A(s) < z_B(s) < z_C(s)$ and with the center of the mass at the origin, i.e.,

$$\sum_{d = A,B,C} m_d z_d(s) = 0. \qquad (24)$$

The Hessian is now block diagonal in x, y, and z with the reaction coordinate and stretching vibrational motions in the z block and the doubly degenerate bending motions in the x and y blocks.

The x block of the Hessian matrix $\mathbf{F}^X(s)$ is defined by

$$F_{dd'}^X(s) = \left(\frac{\partial^2 V}{\partial x_d \partial x_{d'}}\right)\bigg|_{r = a(s)}, \quad d,d' = A,B,C, \qquad (25)$$

where a derivative with respect to a Cartesian coordinate implies that all other Cartesian coordinates are held fixed. To compare with the fixed-bond-length bending frequency, it will be most convenient to express the Hessian matrix in terms of derivatives of the potential with respect to the interbond distances given by

$$R_{dd'}^2 = (x_d - x_{d'})^2 + (y_d - y_{d'})^2$$
$$+ (z_d - z_{d'})^2, \quad d \neq d'. \qquad (26)$$

Along the MEP, $x = y = 0$, therefore, the x block of the Hessian matrix can be rewritten as

$$F_{dd}^X(s) = \sum_{d' \neq d} \frac{1}{R_{dd'}}\left(\frac{\partial V}{\partial R_{dd'}}\right)_{R_{dd''},R_{d'd''}}\bigg|_{r = a(s)}, \qquad (27)$$

$$F_{dd'}^X(s) = -\frac{1}{R_{dd'}}\left(\frac{\partial V}{\partial R_{dd'}}\right)_{R_{dd''},R_{d'd''}}\bigg|_{r = a(s)}, \quad d' \neq d, \qquad (28)$$

where $d'' \neq d$ and $d'' \neq d'$. The mass-weighted Hessian matrix $\mathbf{K}^X$ is then defined by

$$K_{dd'}^X(s) = \frac{\mu}{\sqrt{m_d m_{d'}}} F_{dd'}^X(s). \qquad (29)$$

[To derive Eqs. (27) and (28), we first differentiated the potential with respect to each intratomic distance at fixed value of two others and then computed the second derivatives of the appropriate distance with respect x_d, taking into account that the first derivitives of $R_{dd'}$ with respect to x_d vanish in linear configurations.] At the saddle point or equilibrium geometries, diagonalization of $\mathbf{K}^X$ will yield two zero eigenvectors corresponding to center-of-mass translation and rotation and the eigenvector corresponding to the bending vibration. For arbitrary points along the MEP, it is necessary to constrain the bending motion to be orthogonal to the center-of-mass translational and infinitesimal rotational motions. The normalized eigenvectors for the center-of-mass translation and rotation are given by

$$u_{d,1} \equiv \sqrt{m_d/M}, \quad d = A,B,C, \qquad (30)$$

$$u_{d,2}(s) \equiv \sqrt{m_d/I_0(s)} z_d(s), \quad d = A,B,C, \qquad (31)$$

and the eigenvector for the bending motion can be constructed by requiring it to be orthogonal to $\mathbf{u}_1$ and $\mathbf{u}_2$,

$$\mathbf{u}_3(s) \equiv \mathbf{u}_2(s) \times \mathbf{u}_1. \qquad (32)$$

Substituting Eqs. (30) and (31) into Eq. (32) gives the elements of the normalized vector $\mathbf{u}_3$

$$u_{d,3}(s) = \sqrt{\frac{m_{d'} \cdot m_{d''}}{I_0(s)M}}[z_{d''}(s) - z_{d'}(s)],$$
$$(d,d',d'') = (A,B,C),(B,C,A),(C,A,B). \qquad (33)$$

The bending frequency is then obtained from the expression

$$\mu[\omega_b^{CV}(s)]^2 = [\mathbf{u}_3(s)]^T \mathbf{K}^X(s)\mathbf{u}_3(s). \qquad (34)$$

Substituting Eqs. (27)–(29) and (33) and using the fact that for collinear geometries $R_{dd'} = |z_d - z_{d''}|$ yields

$$[\omega_b^{CV}(s)]^2 = \frac{1}{I_0(s)M}\left[\frac{m_C}{m_B m_A}(m_B R_{BC} + m_A R_{CA})^2 \frac{1}{R_{BA}}\left(\frac{\partial V}{\partial R_{BA}}\right)_{R_{BC}, R_{CA}} + \frac{m_A}{m_B m_C}(m_C R_{CA} + m_C R_{BA})^2\right.$$

$$\left.\times \frac{1}{R_{BC}}\left(\frac{\partial V}{\partial R_{BC}}\right)_{R_{BA}, R_{CA}} + \frac{m_B}{m_C m_A}(m_A R_{BA} + m_C R_{BC})^2 \frac{1}{R_{CA}}\left(\frac{\partial V}{\partial R_{CA}}\right)_{R_{BA}, R_{CA}}\right]\Bigg|_{\mathbf{r} = \mathbf{a}(s)} . \tag{35}$$

This can be rearranged to give

$$[\omega_b^{CV}(s)]^2 = [\omega_b^{BL}(s)]^2 + \frac{1}{I_0(s)Mm_B}\left[\frac{m_C}{m_A R_{BA}}(m_B R_{BC} + m_A R_{CA})^2\left(\frac{\partial V}{\partial R_{AB}}\right)_{R_{BC}, \Phi}\right.$$

$$\left.+ \frac{m_A}{m_C R_{BC}}(m_C R_{CA} + m_B R_{BA})^2\left(\frac{\partial V}{\partial R_{BC}}\right)_{R_{BA}, \Phi}\right]\Bigg|_{\mathbf{r} = \mathbf{a}(s)} , \tag{36}$$

where $\omega_b^{BL}(s)$ is given by Eq. (23) and where we have made use of the relationships

$$\left[\left(\frac{\partial V}{\partial R_{Bd}}\right)_{R_{Bd'}, R_{CA}} = \left(\frac{\partial V}{\partial R_{Bd}}\right)_{R_{Bd'}, \Phi} - \left(\frac{\partial V}{\partial R_{CA}}\right)_{R_{BA}, R_{BC}}\right.$$

$$\left.\times \frac{(R_{Bd'} - R_{Bd'} \cos \Phi)}{R_{CA}}\right] ,$$

$$(d, d') = (A, C) \text{ or } (C, A). \tag{37}$$

At the saddle point the first derivatives in Eq. (36) vanish; therefore, at the saddle point, the bend frequencies computed for the bond-length and Cartesian-vibration reaction coordinates are the same. For arbitrary geometries on the MEP, these two derivatives do not necessarily vanish and the bend frequencies computed for the bond-length and Cartesian-vibration reaction coordinates are not necessarily the same. The connection between Eqs. (14) and (36) will be discussed in the next subsection.

III A 3. Least-squares reaction coordinate and intrabond angle

In the previous section it was shown that the combination of Cartesian-vibration reaction coordinate and Cartesian bending coordinate leads to a different formal expression for the bending frequency than the bond-length reaction coordinate with the intrabond angle used for the bending coordinate. In the present section we wish to show that using different vibrational coordinates with the same reaction coordinate gives the same frequencies. First we note that using the Cartesian-vibration reaction coordinate with Cartesian bending coordinates (the Miller–Handy–Adams procedure) is equivalent to using the least-squares reaction coordinate with a rectilinear bending coordinate.[23] We will show below that the least-squares reaction coordinate combined with intrabond angle (that was used in Sec. III A 1 with the bond-length reaction coordinate) also gives the same frequencies as the Cartesian-vibration reaction coordinate combined with Cartesian bending coordinates.

The Cartesian-vibration reaction coordinate is defined by projecting displacements of the nuclei from the MEP on the subspace of displacements satisfying the Eckart–Sayvetz conditions.[36,37] As a result, both the reaction coordinate s^{CV} and the associated set of Cartesian vibrational coordinates $\mathbf{q}^{CV}$ change when the molecular system rotates as a whole and hence they are not internal coordinates. [Therefore, any true internal variable as well as the potential energy depends not only on $q_1, ..., q_F$, but also on three additional coordinates describing infinitesimal rotations of a structure on the MEP.] Since Eqs. (5), (6), (13), and (14) are strictly applicable only for internal variables, the Miller–Handy–Adams procedure cannot be used without further assumptions. To relate that procedure to the formalism of Sec. II, we make use of the fact that the harmonic vibrational frequencies evaluated with the Miller–Handy–Adams recipe coincide[23] with those calculated using the least-squares reaction coordinate. In the least-squares reaction coordinate system, the molecular system is rotated to satisfy the Eckart–Sayvetz conditions so that s^{LS} is an internal variable by definition. The companion set of rectilinear vibrational coordinates $\mathbf{q}^{LS}$ defined via displacements of the rotated nuclei from the MEP are also internal coordinates. [The least-squares reaction coordinate and rectilinear bend coordinate are defined by Eqs. (4)–(6) in Ref. 39 (with $p = 1$). The two reaction coordinates s^{CV} and s^{LS} coincide in configurations in which nuclear displacements from the MEP satisfy the Eckart–Sayvetz conditions, but they differ from each other everywhere else. The least-squares stretching coordinate will be called q_{str}^{LS}.] Since s^{LS} is an internal coordinate, it can be substituted for other reaction coordinates (whereas s^{CV} can only be used together with the Cartesian vibrations). This property will be convenient to derive the expression for the bending frequency using the least-squares reaction coordinate with the intrabond angle and to show that it is the same as that derived in Sec. III A 2. It is worth noting that one would also get the same harmonic vibrational frequencies by using Basilevsky's natural reaction coordinates[16(a)] [provided that the metric tensor is defined as the inverse of matrix Eq. (6)—compare Ref. 16(b)] because the latter coincide with the least-squares variables in the neighborhood of the MEP.[23]

The least-squares bend frequency in the coordinate system with s^{LS} and the intrabond angle is given by

$$[\omega_b^{LS}(s)]^2 = G_{\Phi\Phi}(s)\left(\frac{\partial^2 V}{\partial \Phi^2}\right)_{s^{LS} = s}\Bigg|_{\mathbf{r} = \mathbf{a}(s)} , \tag{38}$$

where the subscripts on the derivative denote that it is evaluated at a fixed value s of the least-squares reaction coordinate s^{LS} at points on the MEP. The G-matrix element is the same as that used in section III A 1 [see Eq. (16a)], since it follows from the partial derivative relationship between the Cartesian coordinates and the vibrational coordinate, Φ in this case. The second derivative of the potential is expressed in terms of the derivative with respect to the bond coordinates by[38]

$$\left(\frac{\partial^2 V}{\partial \Phi^2}\right)_{s^{LS}=s}\bigg|_{r=a(s)} = F_{\Phi\Phi}(s) + \sum_{d=A,C}\left[\left(\frac{\partial V}{\partial R_{Bd}}\right)_{\Phi,R_{bd'}}\right.$$
$$\left.\times\left(\frac{\partial^2 R_{Bd}}{\partial \Phi^2}\right)_{q_{str}^{LS}=0,s^{LS}=s}\right]\bigg|_{r=a(s)},$$
$$d' \neq d, \qquad (39)$$

where $F_{\Phi\Phi}(s)$ is given by Eq. (16b) and we have made use of the fact that the first derivatives of the bond lengths with respect to Φ, as well as the mixed derivative of the potential with respect to Φ and one of the bond lengths (at fixed values of the two other bond length coordinates) vanish in any linear configuration.

Alternatively, we can represent Eq. (39) by analogy with Eq. (14) as

$$\left(\frac{\partial^2 V}{\partial \Phi^2}\right)_{s^{LS}=s}\bigg|_{r=a(s)} = F_{\Phi\Phi}(s) - b_{\Phi\Phi}(s)$$
$$\times\left(\frac{\partial V}{\partial s^{LS}}\right)_{q_{str}^{LS}=0,\Phi=\pi}\bigg|_{s^{LS}=s}, \qquad (40)$$

where

$$b_{\Phi\Phi}(s) = -\sum_{d=A,C}\left[\left(\frac{\partial s^{LS}}{\partial R_{Bd}}\right)_{\Phi,R_{Bd'}}\right.$$
$$\left.\times\left(\frac{\partial^2 R_{Bd}}{\partial \Phi^2}\right)_{q_{str}^{LS}=0,s^{LS}=s}\right]_{r=a(s)}, \quad d' \neq d, \quad (41)$$

$$\left(\frac{\partial s^{LS}}{\partial R_{BA}}\right)_{\Phi,R_{BC}}\bigg|_{r=a(s)}$$
$$= \frac{\tilde{m}}{\mu}a^{-2}\left[\left(\frac{\partial R_{BA}}{\partial s^{LS}}\right)_{q_{str}^{LS}=0,\Phi=\pi}\right.$$
$$\left.+\frac{m_C}{(m_B+m_C)}\left(\frac{\partial R_{BC}}{\partial s^{LS}}\right)_{q_{str}^{LS}=0,\Phi=\pi}\right], \qquad (42a)$$

$$\left(\frac{\partial s^{LS}}{\partial R_{BC}}\right)_{\Phi,R_{BA}}\bigg|_{r=a(s)}$$
$$= \frac{\tilde{m}}{\mu}\left[a^{-2}\frac{m_C}{m_B+m_C}\left(\frac{\partial R_{BA}}{\partial s^{LS}}\right)_{q_{str}^{LS}=0,\Phi=\pi}\right.$$
$$\left.+\left(a^2+a^{-2}\frac{m_C^2}{(m_B+m_C)^2}\right)\left(\frac{\partial R_{BC}}{\partial s^{LS}}\right)_{q_{str}^{LS}=0,\Phi=\pi}\right], \qquad (42b)$$

and[34]

$$a = [Mm_Bm_C/m_A(m_B+m_C)^2]^{1/4}. \qquad (43)$$

Explicit expressions for the second derivatives of the bond lengths R_{BA} and R_{BC} with respect to Φ in Eqs. (39) and (41) will be given below.

One of the major difficulties in determining the least-squares bend frequency in these coordinates is the evaluation of derivatives with respect to Φ explicitly keeping fixed the least-squares reaction coordinate. This can be accomplished by the least-squares algorithm[23] or through the first-order differential equations following from the Eckart–Sayvetz conditions.[36,37] For a triatomic with a collinear MEP, the Sayvetz condition which requires displacements along vibrational coordinates to be orthogonal to the reaction coordinate can be written as

$$\sum_{d=A,B,C}m_d\frac{dz_d}{ds}[z_d^{LS}-z_d(s)] = 0, \qquad (44a)$$

where z_d^{LS} is the projection of nucleus d on the z axis of the least-squares body-fixed frame for a displacement from the MEP along a vibrational coordinate. For the bending coordinate, Eq. (44a) is satisfied if z_d^{LS} does not change from the reaction-path value $z_d(s)$ for a bending motion, i.e.,

$$\left(\frac{\partial z_d^{LS}}{\partial \Phi}\right)_{s^{LS}=s} = 0, \quad d=A,B,C. \qquad (44b)$$

This also implies that the stretching vibrational coordinate q_{str}^{LS} remains identically zero for a bend. The Eckart condition requires displacements along vibrational coordinates to be orthogonal to infinitesimal rotations and for the triatomic system consider here, it can be rewritten as

$$\sum_{d=A,B,C}m_d z_d(s)x_d^{LS} = 0, \qquad (44c)$$

where x_d^{LS} is defined in a manner analogous to z_d^{LS}.

The bond lengths are defined in terms of the Cartesian variables by Eq. (26) which for bending displacements in the x direction can be expressed as

$$R_{Bd}^2 = (x_{Bd}^{LS})^2 + (z_{Bd}^{LS})^2, \qquad (44d)$$

where $x_{Bd}^{LS} = x_d^{LS} - x_B^{LS}$ and $z_{Bd}^{LS} = z_d^{LS} - z_B^{LS}$. Using Eq. (44b) and the fact that x_{Bd}^{LS} vanishes in any collinear configuration results in

$$\left(\frac{\partial^2 R_{Bd}}{\partial \Phi^2}\right)_{s^{LS}=s}\bigg|_{r=a(s)} = \left[\frac{1}{R_{Bd}}\left(\frac{\partial x_{Bd}}{\partial \Phi}\right)^2_{s^{LS}=s}\right]\bigg|_{r=a(s)} \qquad (44e)$$

and it only remains to evaluate the derivative of the Cartesian coordinates x_{Bd}^{LS} with respect to Φ. This is accomplished using the Eckart condition (44c) and by requiring the center of mass to remain stationary during the bending, e.g., Eq. (24).

Differentiation of the Eckart condition (44c) with respect to Φ leads to one equation for the first derivative of x_d^{LS} with respect to Φ

$$\sum_{d=A,B,C}m_d z_d(s)\left(\frac{\partial x_d^{LS}}{\partial \Phi}\right)_{s^{LS}=s}\bigg|_{r=a(s)} = 0. \qquad (45)$$

Using Eq. (24) we can also write this relation as

$$\sum_{d=A,C}m_d z_d(s)\left(\frac{\partial x_{Bd}^{LS}}{\partial \Phi}\right)_{s^{LS}=s}\bigg|_{r=a(s)} = 0. \qquad (46)$$

A second relationship for $\partial x_{Bd}^{LS}/\partial \Phi$ can be obtained by differentiating the vector cross product equation

$$(\mathbf{R}_{BA} \times \mathbf{R}_{BC})_y \equiv x_{BC}^{LS} z_{BA}^{LS} - x_{BA}^{LS} z_{BC}^{LS} = R_{BA} R_{BC} \sin \Phi \tag{47}$$

with respect to Φ and putting $\Phi = \pi$, to yield

$$\left[\frac{1}{R_{BA}} \left(\frac{\partial x_{BA}^{LS}}{\partial \Phi} \right)_{s^{LS} = s} \right] \Bigg|_{\mathbf{r} = \mathbf{a}(s)} = 1. \tag{48}$$

Solving Eqs. (46) and (48) we obtain

$$\left(\frac{\partial x_{BA}^{LS}}{\partial \Phi} \right)_{s^{LS} = s} \Bigg|_{\mathbf{r} = \mathbf{a}(s)}$$

$$= \left[\frac{\epsilon_d m_{d'} z_{d'}(s) R_{BA} R_{BC}}{I_0(s)} \right] \Bigg|_{\mathbf{r} = \mathbf{a}(s)},$$

$$(d, d') = (A, C) \text{ or } (C, A), \tag{49}$$

where

$$\epsilon_A = 1, \quad \epsilon_C = -1. \tag{50}$$

Use was also made of the relationship for the moment of inertia for collinear geometries

$$I_0 = [m_C z_C(s) R_{BC} - m_A z_A(s) R_{BA}]|_{\mathbf{r} = \mathbf{a}(s)}, \tag{51}$$

which is a result of Eq. (24).

Combining Eqs. (15), (16), (38), (39), (44e), (49), and (51) leads to the desired expression for the least-squares bending frequency in this coordinate system,

$$[\omega_b^{LS}(s)]^2 = [\omega_b^{BL}(s)]^2 + \frac{1}{\bar{m}^2 I_0(s)} \sum_{d = A, C} m_d^2 z_d^2(s) v_d, \tag{52}$$

where

$$v_d \equiv \left[\frac{1}{R_{Bd'}} \left(\frac{\partial V}{\partial R_{Bd'}} \right)_{\Phi, R_{Bd}} \right] \Bigg|_{\mathbf{r} = \mathbf{a}(s)},$$

$$(d, d') = (A, C) \text{ or } (C, A). \tag{53}$$

Equation (52) is an alternative expression of Eq. (36) and it shows again that by requiring that s^{LS} instead of s^{BL} remains fixed during bending displacements, one obtains a different bending frequency even though the bending coordinate is the same. However, the least-squares bending frequency obtained in Eq. (52) is identical to that given above in Eq. (36). This can be shown by using Eq. (37). Thus, the bending frequency does not depend on the choice of bending coordinate, although it does depend on the definition of the reaction coordinate.

III B. Reaction $CH_3 + H_2 \rightarrow CH_4 + H$ along a C_{3v} reaction path

Reaction (R3) gives us an example of a polyatomic system for which, due to the C_{3v} symmetry of the MEP, we may make interesting analogies to a triatomic reactions with a collinear MEP. The reaction coordinate in this case is a function of *totally symmetric* (TS) vibrational coordinates $\bar{q}_j^{TS}$ ($j = 1, 2, ..., N - 2$; where N is the number of atoms) such

that their *infinitesimal* deviations for any C_{3v} configuration retain the symmetry. The *infinitesimal* deviations of *symmetry-breaking* (SB) coordinates q_j^{SB} may be chosen to span the two-dimensional irreducible representations of the C_{3v} group. Like the collinear triatomic MEP, the reaction coordinate for (R3) is a totally symmetric coordinate and, hence, the coefficients of momentum coupling between the motion along the path and symmetry-breaking vibrations vanish in any C_{3v} configuration, i.e.,

$$\sum_d \frac{1}{m_d} \left[\frac{\partial s}{\partial \mathbf{r}_d} \cdot \frac{\partial q_j^{SB}}{\partial \mathbf{r}_d} \right] \Bigg|_{\mathbf{r} = \mathbf{a}(s)} = 0, \quad j = 1, 2, ..., 2N - 4. \tag{54}$$

But we still must enforce $G_{iF} = 0$ for i corresponding to a totally symmetric coordinate by the proper choice of these coordinates [see Eq. (6)].

For C_{3v} symmetry the GF matrix takes a block diagonal form and we can consider separately the subspaces of totally symmetric and symmetry-breaking vibrational coordinates. In particular, for reaction (R3) we have three totally symmetric vibrational coordinates and four pairs of doubly degenerate symmetry-breaking vibrational coordinates. We consider two different reaction coordinates which are defined in exactly the same way in the subspace of C_{3v} configurations and, as a result, only the harmonic frequencies in the symmetry-breaking subspace change with different choices of the "totally symmetric" reaction coordinate. Thus, the symmetry-breaking subspace is analogous to the bending modes of the collinear atom–diatom complexes. Therefore, for any new definition of the reaction coordinate, the first problem is how to evaluate the second derivatives of the potential with respect to the symmetry-breaking coordinates for fixed values of the selected totally symmetric coordinates. To evaluate the frequencies, we also need to compute the G matrix elements.

Two choices of the reaction coordinate are described in this section. The first reaction coordinate, which is new and is described in Sec. III B 1, involves Cartesian-vibrational coordinates defined in the Eckart frame attached to the methyl hydrogens. This treatment differs from the treatments of Refs. 21 and 23 by the choice of directions in which the system distorts with a constant value of the reaction coordinate. In the present treatment, the Eckart frame of the methyl hydrogens is held fixed when vibrational coordinates are varied. Because of the prominent role which totally symmetric Cartesian vibrations measured relative to the Eckart frame of the methyl hydrogens play in the resulting transformations, the reaction coordinate defined by this transformation is called the methyl-Eckart-frame Cartesian-vibration (MEF–CV) reaction coordinate. It is denoted $\bar{s}$. (In this section we reserve s for the reaction coordinate on the MEP and in other C_{3v} geometries, where both definitions agree.)

The second treatment is also new and it defines the reaction coordinate for non-C_{3v} configurations in terms of curvilinear coordinates corresponding to fixing the bond lengths of the making and breaking bonds when the system distorts with a constant value of the reaction coordinate. This defines the bond-length reaction coordinate or s^{BL}. The computation of the necessary quantities for the bond-length reaction

coordinate in Sec. III B 2 is based on the set of totally symmetric coordinates introduced at the end of Sec. III B 1. The main advantage of this set of vibrational variables is that the second derivatives of the potential can be easily evaluated in this coordinate system. In Sec. III B 2, we the use the chain rule to calculate the necessary second derivatives at fixed values of the bond lengths R_{CH} and $R_{HH'}$, where H and H' are the hydrogens forming the hydrogen molecule with H' taken to be the hydrogen atom furthest from the carbon. The second derivatives are calculated with two other totally symmetric coordinates kept fixed, the height of the CH_3 pyramid, and the totally symmetric Cartesian-vibrational coordinate of the isolated CH_3 radical.

III B 1. Methyl-Eckart-frame Cartesian-vibration reaction coordinate

In this section we define the reaction coordinate using Cartesian coordinates of the three reacting atoms (C, H, and H') in a body-fixed frame attached to the methyl hydrogens. Although the treatment is applicable to an arbitrary reaction of the form $CX_3 + YZ$, as long as the MEP has C_{3v} symmetry, we use the notation $CH_aH_bH_c + HH'$ $\rightarrow CH_aH_bH_cH + H'$ for concreteness and to avoid confusion with the X, Y, and Z Cartesian directions. We place the triangle $H_aH_bH_c$ of the CH_3 pyramid in the XY plane of a body-fixed XYZ coordinate frame with the $H_aH_bH_c$ center-of-mass at the origin. We use the Cartesian normal coordinates Q_1, Q_{2X}, and Q_{2Y} of the hydrogens in the planar CH_3 molecule to describe vibrations in the triatom, with Q_1 being the CH_3 breathing mode and with Q_{2X} and Q_{2Y} being symmetric with respect to reflections in the XZ and YZ planes, respectively. The other vibrational coordinates are taken to be the Cartesian coordinates of C, H, and H' in the same body-fixed frame; i.e., X_C, Y_C, Z_C, X_H, Y_H, Z_H, $X_{H'}$, $Y_{H'}$, $Z_{H'}$. The change of variables just described is closely related to that suggested by Wallace,[40] except that we measure overall rotations and vibrations of the triatom $H_aH_bH_c$ relative to the Eckart frame,[36] whereas according to Wallace's recipe they would be measured relative to the atom–diatom body-fixed frame of Curtiss, Hirschfelder, and Adler.[41]

The space-fixed coordinate vectors of the C, H, and H' atoms are denoted r_d, $d = C, H, H'$; and r_α ($\alpha = a,b,c$) is specifically used when we wish to refer only to the space-fixed coordinate vectors of H_α ($\alpha = a,b,c$). The following transformation leads from the coordinate system just described to the space-fixed atomic coordinate vectors

$$r_d = r_\Delta + S(\phi,\theta,\psi)\begin{pmatrix} X_d \\ Y_d \\ Z_d \end{pmatrix}, \quad d = C,H,H' \qquad (55)$$

$$r_\alpha = r_\Delta + S(\phi,\theta,\psi)\left[r_\alpha^e + c_\alpha^Z Q_1 + \sum_{K=X,Y} c_\alpha^K Q_{2K} \right],$$
$$\alpha = a,b,c, \qquad (56)$$

where r_Δ is the coordinate vector of the center-of-mass of the $H_aH_bH_c$ triangle, r_α^e is the coordinate vector of a hydrogen in the equilibrium configuration of the planar CH_3 radical

(with H_a on the X axis), and $S(\phi,\theta,\psi)$ is the direction cosine matrix of the Eckart frame attached to the triangle $H_aH_bH_c$ and described by three Euler angles ϕ, θ, and ψ. The coefficients c_α^K in Eq. (56) are given by the relations

$$c_\alpha^K = \frac{1}{\sqrt{3}} \left.\frac{\partial S_{2K}}{\partial r_\alpha}\right|_{r=r^e}, \quad K = X,Y \quad \text{and} \quad \alpha = a,b,c \qquad (57)$$

$$c_\alpha^Z = \frac{1}{\sqrt{3}} \hat{r}_\alpha^e, \quad \alpha = a,b,c \qquad (58)$$

with

$$S_{2X} = \sqrt{\frac{2}{3}} \left[\frac{1}{2} (R_{ab} + R_{ac}) - R_{bc} \right], \qquad (59)$$

$$S_{2Y} = \frac{1}{\sqrt{2}} (R_{ab} - R_{ac}), \qquad (60)$$

and

$$\hat{r}_\alpha^e = r_\alpha^e / r_{CH}^e, \quad \alpha = a,b,c, \qquad (61)$$

where r_{CH}^e and $R_{\alpha\alpha'}$ denote, respectively, the CH bond length in the equilibrium configuration of the planar CH_3 radical and the interatomic distance between hydrogens H_α and $H_{\alpha'}$ in an arbitrary configuration. Substituting Eqs. (59) and (60) into (57) and using the relation

$$\left.\frac{\partial R_{\alpha\alpha'}}{\partial r_\alpha}\right|_{r=r^e} = \delta_{\alpha\alpha''} \hat{r}_{\alpha'\alpha}^e + \delta_{\alpha'\alpha''} \hat{r}_{\alpha\alpha'}^e,$$
$$\alpha,\alpha' = a,b,c \qquad (62)$$

with

$$\hat{r}_{\alpha'\alpha}^e \equiv (r_\alpha^e - r_{\alpha'}^e)/|r_\alpha^e - r_{\alpha'}^e|$$
$$= \frac{1}{\sqrt{3}r_{CH}^e}(r_\alpha^e - r_{\alpha'}^e), \quad \alpha,\alpha' = a,b,c \qquad (63)$$

leads to

$$\frac{3}{2} c_a^X = \frac{1}{2}(\hat{r}_{ba}^e + \hat{r}_{ca}^e), \quad c_a^Y = \frac{1}{\sqrt{3}}\hat{r}_{bc}^e, \qquad (64),(65)$$

$$\frac{3}{2} c_b^X = \frac{1}{2}\hat{r}_{ab}^e - \hat{r}_{cb}^e, \quad c_b^Y = \frac{1}{\sqrt{3}}\hat{r}_{ab}^e, \qquad (66),(67)$$

$$\frac{3}{2} c_c^X = \frac{1}{2}\hat{r}_{ca}^e - \hat{r}_{bc}^e, \quad c_c^Y = \frac{1}{\sqrt{3}}\hat{r}_{ca}^e. \qquad (68),(69)$$

Taking into account that

$$\hat{r}_{\alpha\alpha'}^e \cdot \hat{r}_{\alpha''\alpha'}^e = \begin{cases} -1 & \alpha = \alpha', \\ -\frac{1}{2} & \alpha \neq \alpha', \end{cases} \qquad (70)$$

one can directly verify that the coefficients c_α^K satisfy the Eckart conditions:

$$\sum_{\alpha=a}^c c_\alpha^K = 0 \qquad (71)$$

$$\sum_{\alpha=a}^c r_\alpha^e \times c_\alpha^K = 0 \qquad (72)$$

together with the normalizing relation:

$$\sum_{i=a}^{c} \mathbf{c}_\alpha^K \cdot \mathbf{c}_\alpha^{K'} = \delta_{KK'}. \tag{73}$$

We can now specify the configuration of CH_5 by the following set of twelve Cartesian vibrational coordinates:

$$\bar{F}_{tt'}^K = \tilde{F}_{t't}^K = \begin{cases} H_{tK,t'K} & t,t' = C,H,H' \\[2mm] \displaystyle\sum_{\substack{\alpha' = a,b,c \\ K' = X,Y}} c_{\alpha',K'}^K \cdot H_{tK,\alpha'K'} & t = C,H,H';t' = 0 \\[3mm] \displaystyle\sum_{\substack{\alpha',\alpha'' = a,b,c \\ K',K'' = X,Y}} c_{\alpha',K'}^K \cdot c_{\alpha'',K''}^K \cdot H_{\alpha'K',\alpha''K''} & t,t' = 0 \end{cases}, \tag{74}$$

where the elements $H_{dK,d'K'}$ of the Hessian matrix are the second derivatives of the potential V with respect to the Cartesian coordinates of the nuclei at the appropriate point of the reaction path. The notation $H_{\alpha K,dK'}$ indicates derivatives with respect to $r_{\alpha K}$ and $r_{d'K'}$ where $\alpha = a,b,c$ refer to atoms H_a, H_b, H_c, and $d = C, H, H'$. Note that the elements of the $\tilde{F}^K$ matrix with subscript 0 refer to derivative of the potential with respect to the vibrational coordinates Q_{2X}, Q_{2Y}, and Q_1, for $K = X, Y, Z$, respectively.

To find the $\mathbf{G}$ matrix, it is convenient to measure the body-fixed projections of the nuclei $C, H,$ and H' from the center of the total nuclear mass. Then

$$\mathbf{r}^{CM} = \mathbf{r}_\Delta + \mathbf{S}(\phi,\theta,\psi)\mathbf{R}, \tag{75}$$

with

$$\mathbf{R} = \begin{pmatrix} X \\ Y \\ Z \end{pmatrix} = \frac{1}{M}\left[m_C \begin{pmatrix} X_C \\ Y_C \\ Z_C \end{pmatrix} + m_H \begin{pmatrix} X_H + X_{H'} \\ Y_H + Y_{H'} \\ Z_H + Z_{H'} \end{pmatrix} \right] \tag{76}$$

and $M = m_C + 5m_H$. The transformation Eqs. (55) and (56) then takes the form

$$\mathbf{r}_d = \mathbf{r}^{CM} + \mathbf{S}(\phi,\theta,\psi)\begin{pmatrix} X_d - X \\ Y_d - Y \\ Z_d - Z \end{pmatrix}, \quad d = C,H,H' \tag{77}$$

$$\mathbf{r}_\alpha = \mathbf{r}^{CM} + \mathbf{S}(\phi,\theta,\psi)\left[\mathbf{r}_\alpha^e - \mathbf{R} + \mathbf{c}_\alpha^Z Q_1 + \sum_{K=X,Y} \mathbf{c}_\alpha^K Q_{2K} \right],$$

$$\alpha = a,b,c. \tag{78}$$

The $\mathbf{G}$ matrix for the space of all vibrational variables is block diagonal with a 4×4 block for totally symmetric coordinates and two 4×4 blocks for symmetry-breaking coordinates. Furthermore, each block factors into a 3×3 block and a diagonal element determining the kinetic energy of the appropriate vibrational motion in the $H_a H_b H_c$ triangle. In principle, the elements of the $\mathbf{G}$ matrix should be found using Eq. (6). However, for the present Cartesian-vibrational variables defined by means of a body-fixed frame, the resultant expressions can be much easier obtained by inverting the $(3N-3) \times (3N-3)$ matrix formed by the coefficients of

$\{r_{tK}\}_{t=C,H,H';K=X,Y,Z}$, $r_{0X} \equiv Q_{2X}$, $r_{0Y} \equiv Q_{2Y}$, and $r_{0Z} = Q_1$. Differentiating the potential V with respect to these vibrational coordinates at fixed values of $\mathbf{r}_\Delta$ and the Euler angles ϕ, θ, and ψ, we obtain three 4×4 matrix blocks $\tilde{F}^X$, $\tilde{F}^Y$, and $\tilde{F}^Z$ with the elements

the components of angular velocity vector and velocities of vibrational motions in the classical kinetic energy. These coefficients can be easily calculated for the body-fixed frame used to define the vibrational coordinates. After the matrix formed by these coefficients is inverted, one simply needs to select its block describing momentum coupling in the space of vibrational motions. For totally symmetric modes, one simply needs to invert the 3×3 block $\tilde{T}^Z$ with the elements

$$\tilde{T}_{dd'}^Z = \begin{cases} m_d(M - m_d)/M & d = d' \\ -m_d m_{d'}/M & d \neq d' \end{cases} \quad d,d' = C,H,H'. \tag{79}$$

Since (in contrast to the least-squares set of variables) symmetry-breaking nuclear displacements in the body-fixed frame in question do not satisfy the Eckart conditions along the MEP, velocity coupling between overall rotations and symmetry-breaking coordinates should be taken into consideration. Hence, the matrix of velocity coupling is 5×5 with a diagonal element for the Q_{2X} or Q_{2Y} motion and a 4×4 block which contains the rotational coupling:

$$\mathbf{T}^X = \mathbf{T}^Y = \begin{pmatrix} \tilde{\mathbf{T}}^Z & \mathbf{t}^+ \\ \mathbf{t} & I_\perp \end{pmatrix}, \tag{80}$$

with

$$t_d = -m_d(Z_d - Z), \quad d = C,H,H' \tag{81}$$

and $I_\perp$ used for the moment inertia of the C_{3v} configuration in question relative to its symmetry axis. The block of the $\mathbf{G}$ matrix sought for can be then represented as

$$\tilde{\mathbf{G}}^X = \tilde{\mathbf{G}}^Y = \begin{pmatrix} m_H^{-1} & \mathbf{0} \\ \mathbf{0}^T & \tilde{\mathbf{G}}^{(1)} \end{pmatrix} \equiv \tilde{\mathbf{G}}^\perp, \tag{82}$$

where $\mathbf{0}$ is the 3×1 null matrix, $\mathbf{0}^T$ is its transpose, and $\tilde{\mathbf{G}}^{(1)}$ is formed by the first three rows and columns of the inverse matrix of Eq. (80). We calculate the harmonic frequencies of symmetry-breaking modes by diagonalizing the symmetric 4×4 matrix $(\tilde{\mathbf{G}}^\perp)^{1/2}\tilde{\mathbf{F}}^\perp(\tilde{\mathbf{G}}^\perp)^{1/2}$ with $\tilde{\mathbf{F}}^\perp \equiv \tilde{\mathbf{F}}^X = \tilde{\mathbf{F}}^Y$ as defined in Eq. (74) with $K = X$ or Y.

We have provided expressions for obtaining the harmonic frequencies for the symmetry-breaking vibrations without giving the explicit definition of the reaction coordi-

nate. We do not need to define these coordinates to obtain the MEF–CV vibrational frequencies for the totally symmetric vibrations since the totally symmetric frequencies do not change with different choices of totally symmetric reaction coordinate and they can be computed more easily by the Miller–Handy–Adams projection technique. However, we will need these coordinates in the next subsection, and so we close the present subsection with their definition; we illustrate their use by giving a prescription for using them to obtain the frequencies of the totally symmetric vibrations.

To define the reaction coordinate $\bar{s}$ and the set of totally symmetric vibrational coordinates $\tilde{q}_j^{TS}$ ($j = 1,2,3$), we introduce an intermediate set of three mass-scaled Jacobi coordinates by analogy with the atom–diatom coordinates of Marcus,[5] in particular,

$$\eta_1 = \sqrt{\mu_1/\mu} Z_C, \tag{83}$$

$$\eta_2 = \sqrt{\mu_2/\mu}[m_C Z_C/m_2 - Z_H], \tag{84}$$

$$\eta_3 = \sqrt{\mu_3/\mu}[(m_C Z_C + m_H Z_H)/m_3 - Z_{H'}] \tag{85}$$

with

$$m_2 \equiv m_C + m_A, \quad m_3 \equiv m_2 + m_H, \quad m_A = 3m_H \tag{86}$$

and

$$\mu_1 \equiv m_C m_A/m_2, \quad \mu_2 \equiv m_H m_2/m_3, \quad \mu_3 \equiv m_H m_3/M. \tag{87}$$

The four totally symmetric degrees of freedom are described by Eqs. (83)–(85) and the vibrational coordinate

$$\eta_0 \equiv \sqrt{m_H/\mu} Q_1. \tag{88}$$

The methyl-Eckart-frame Cartesian-vibration reaction coordinate $\bar{s}$ and three totally symmetric vibrational coordinates $\tilde{q}_j^{TS}$ ($j = 1,2,3$) are then defined by the implicit relations

$$\eta_k(\bar{s}, \tilde{\mathbf{q}}^{ST}) = \eta_k^{(0)}(\bar{s}) + \sum_{j=1}^{3} \tilde{c}_{kj}^{TS}(\bar{s}) \tilde{q}_j^{TS} \quad k = 0,1,2,3, \tag{89}$$

where the coordinates η evaluated on the reaction path are defined in terms of the reaction-path coordinates of Eq. (2) by

$$\eta_0^{(0)}(s) \equiv (m_H/\mu)^{1/2}(m_H^{-1/2} a_{H_a X}(s) - r_{CH}^e), \tag{90}$$

$$\eta_1^{(0)}(s) = (\mu_1/\mu)^{1/2}(m_C^{-1/2} a_{CZ}(s) - m_H^{-1/2} a_{H_a Z}(s)), \tag{91}$$

$$\eta_2^{(0)}(s) = (\mu_2/\mu)^{1/2}\left[(m_A m_H^{-1/2} a_{H_a Z}(s) + m_C^{1/2} a_{CZ}(s))/m_2 - m_H^{-1/2} a_{HZ}(s)\right], \tag{92}$$

$$\eta_3^{(0)}(s) = (\mu_3/\mu m_H)^{1/2}\{[m_A a_{H_a Z}(s) + (m_H m_C)^{1/2} \times a_{CZ}(s) + m_H a_{HZ}(s)]/m_3 - a_{H'Z}(s)\}. \tag{93}$$

Since the MEP is the path of steepest descent in mass-scaled Cartesian coordinates, we have

$$\sum_d \left|\frac{d\mathbf{a}_d}{ds}\right|^2 = 1, \tag{94}$$

where μ is the reduced mass of Eq. (1). Therefore,

$$\sum_{t=0}^{3} \left(\frac{d\eta_t^{(0)}}{ds}\right)^2 \equiv 1. \tag{95}$$

The coefficients $\tilde{c}^{TS}$ of the transformation within the totally symmetric space of coordinates are defined by

$$\tilde{c}_{kj}^{TS}(\bar{s}) = \frac{\partial \eta_k}{\partial \tilde{q}_j^{TS}}, \quad k = 0,1,2,3; \ j = 1,2,3 \tag{96}$$

and are orthogonal to the gradient along the MEP expressed in these vibrational coordinates

$$\sum_{k=0}^{3} \frac{d\eta_k^{(0)}}{ds} \tilde{c}_{kj}^{TS}(\bar{s}) \equiv 0, \quad j = 1,2,3. \tag{97}$$

In addition, since the vibrational coordinates $\tilde{\mathbf{q}}^{TS}$ describe generalized normal modes, we require that

$$\left[\frac{1}{\mu} \sum_{k,k'=0}^{3} \tilde{c}_{kj}^{TS}(s) F_{kk'}^{\eta}(s) \tilde{c}_{k'j}^{TS}(s) - \omega_j^2(s)\delta_{jj'}\right] = 0, \quad j = 1,2,3, \tag{98}$$

where the force constant matrix in the vibrational coordinates η is defined by

$$F_{kk'}^{\eta}(s) \equiv \sum_{t,t'=0,C,H,H',A} W_{tt'}^{\|} \frac{\partial \zeta_t}{\partial \eta_k} \frac{\partial \zeta_{t'}}{\partial \eta_{k'}},$$
$$k,k' = 0,1,2,3. \tag{99}$$

In Eq. (99) we have introduced a new set of coordinates ζ that include four totally symmetric vibrational degrees of freedom and overall translation along the C_{3v} symmetry axis. These coordinates are given by

$$\zeta_0 \equiv \sqrt{m_0/\mu} Q_1 = \eta_0, \tag{100}$$

$$\zeta_t = \sqrt{m_t/\mu}(r_A + Z_t), \quad t = C,H,H' \tag{101}$$

$$\zeta_A = \sqrt{m_A/\mu} r_A, \tag{102}$$

where $m_0 \equiv m_H$, and r_A is the space-fixed z coordinate of the center-of-mass of the triangle $H_a H_b H_c$ in an arbitrary C_{3v} configuration of the whole system. The symmetric matrix of second derivatives in these new coordinates is given by

$$\sqrt{\frac{m_t m_{t'}}{\mu}} W_{tt'}^{\|}$$

$$= \begin{cases} \tilde{F}_{tt'}^{Z}, & t,t' \neq A \\ \sum_{\alpha'=a,b,c} H_{tK',\alpha Z}, & t \neq 0,A, \ t' = A \\ \sum_{\substack{\alpha',\alpha''=a,b,c \\ K=X,Y}} H_{\alpha'K,\alpha''Z} c_{\alpha'K}^{Z}, & t = 0, \ t' = A \\ \sum_{\alpha',\alpha''=a,b,c} H_{\alpha'Z,\alpha''Z}, & t = t' = A \end{cases}, \tag{103}$$

where $\tilde{\mathbf{F}}^Z$, $\mathbf{H}$, and $\mathbf{c}^Z$ are defined above. Instead of solving Eq. (98) under conditions in Eq. (97), it is convenient to apply a projection technique (which is a modification of that introduced by Miller, Handy, and Adams[21]) to the five-dimensional system described by the mass-scaled Cartesian coordinates ζ. The potential function is invariant under translation of only four masses—C,H,H', and the center-of-mass of the

triangle (Δ); overall translation does not depend on the vibrational motion Q_1 (or $\eta_0 = \zeta_0$). As a result, the eigenvector of the 5×5 matrix $\mathbf{W}^{\parallel}$ corresponding to the zero eigenvalue has the form

$$\bar{e} = (0 \quad \sqrt{m_C/M} \quad \sqrt{m_H/M} \quad \sqrt{m_{H'}/M} \quad \sqrt{m_\Delta/M}).$$
(104)

Since the coordinates η_0, η_1, η_2, and η_3 determine the 4-dimensional hyperplane orthogonal to the vector in Eq. (104) defined in the space of coordinates in Eqs. (100)–(102), and since the coefficients $\bar{c}^{TS}$ are orthogonal to the gradient of the potential [see Eq. (97)], the projector in question can be represented as

$$P_{tt'} = \delta_{tt'} - (1 - \delta_{t0})(1 - \delta_{t'0}) \frac{\sqrt{m_t m_{t'}}}{M}$$

$$- \frac{d\zeta_t^{(0)}}{ds} \frac{d\zeta_{t'}^{(0)}}{ds}, \quad t, t' = 0, C, H, H', \Delta, \quad (105)$$

with

$$\zeta_0^{(0)}(s) = (m_\Delta/\mu)^{1/2}(m_H^{-1/2} a_{H_a X}(s) - r_{CH}^e), \quad (106)$$

$$\zeta_t^{(0)}(s) = \mu^{-1/2} a_{tZ}(s), \quad t = C, H, H', \quad (107)$$

$$\zeta_\Delta^{(0)}(s) = (m_\Delta/\mu m_H)^{1/2} a_{H_a Z}(s). \quad (108)$$

The harmonic frequencies of the totally symmetric normal modes calculated in such a way coincide with the harmonic frequencies of the *nondegenerate* normal modes obtained by applying the Miller–Handy–Adams technique to the full 18-dimensional space of the reaction (R3).

III B 2. Bond-length reaction coordinate

We now introduce a new "bond-length" reaction coordinate s^{BL} defined as a function of the CH_3 breathing mode Q_1 and three *geometrical* vibrational coordinates—the height Z_C of the CH_3 pyramid and two bond lengths R_{CH} and $R_{HH'}$—in such a way that s^{BL} coincides with $\bar{s}$ in any C_{3v} configuration. This implies that we first express Z_H and $Z_{H'}$ in terms of the coordinates $Z_{H'}$-Z_H, Z_H-Z_C, and Z_C, and then substitute $Z_{H'}$-Z_H and Z_H-Z_C in the resultant expression for the bond lengths $R_{HH'}$ and R_{CH}. The new coordinates η_0, η_1, η_2, η_3, obtained in such a way are connected with the new reaction coordinate s^{BL} and the associated totally symmetric Cartesian-vibrational coordinates q_1^{TS}, q_2^{TS}, q_3^{TS} by means of relations in Eq. (89) with s^{BL}, $\mathbf{q}^{TS}$ used instead of $\bar{s}$, $\bar{\mathbf{q}}^{TS}$. Therefore, the harmonic frequencies of totally symmetric vibrations calculated with this new definition of the reaction coordinate are exactly the same as those calculated using the Cartesian-vibration reaction coordinate, e.g., by the Miller–Handy–Adams projection technique. The choice of the vibrational coordinates does not affect the harmonic frequencies so we keep all the symmetry-breaking coordinates Q_{2X}, Q_{2Y}, and X_d, Y_d ($d = C, H, H'$) the same because they are convenient for calculations of all the necessary second derivatives. The immediate consequence of such a choice of the vibrational coordinates is that the appropriate block of the $\mathbf{G}$ matrix also remains the same.

To calculate the second derivatives of the potential at fixed values of the new totally symmetric vibrational coordi-

nates, one needs to compute the second derivatives of Z_H and $Z_{H'}$ with respect to Q_{2X}, Q_{2Y} and X_d, Y_d ($d = C, H, H'$) at fixed values of Q_1, Z_C, R_{CH}, and $R_{HH'}$. One finds

$$Z_H = Z_C + \sqrt{R_{CH}^2 - (X_C - X_H)^2 - (Y_C - Y_H)^2},$$
(109)

$$Z_{H'} = Z_H + \sqrt{R_{HH'}^2 - (X_H - X_{H'})^2 - (Y_H - Y_{H'})^2}$$
(110)

and hence the X and Y blocks of the $\mathbf{F}$ matrix in question have the following form:

$$F_{CC}^{\perp} \equiv \tilde{F}_{CC}^{\perp} - \frac{1}{R_{CH}} \frac{\partial V}{\partial Z_H}, \quad (111)$$

$$F_{HH}^{\perp} \equiv \tilde{F}_{HH}^{\perp} - \frac{1}{R_{CH}} \frac{\partial V}{\partial Z_H} - \frac{1}{R_{HH'}} \frac{\partial V}{\partial Z_{H'}}, \quad (112)$$

$$F_{H'H'}^{\perp} \equiv \tilde{F}_{H'H'}^{\perp} - \frac{1}{R_{HH'}} \frac{\partial V}{\partial Z_{H'}}, \quad (113)$$

$$F_{CH}^{\perp} \equiv \tilde{F}_{CH}^{\perp} + \frac{1}{R_{CH}} \frac{\partial V}{\partial Z_H}, \quad (114)$$

$$F_{HH'}^{\perp} \equiv \tilde{F}_{HH'}^{\perp} + \frac{1}{R_{HH'}} \frac{\partial V}{\partial Z_{H'}}, \quad (115)$$

$$F_{dd'}^{\perp} \equiv \tilde{F}_{dd'}^{\perp} \quad (116)$$

for all other combinations of d and d' where $\mathbf{F}^{\perp} = \mathbf{F}^X = \mathbf{F}^Y$. We calculate the new harmonic frequencies of symmetry-breaking modes by diagonalizing the symmetric 4×4 matrix $(\tilde{\mathbf{G}}^{\perp})^{1/2} \mathbf{F}^{\perp} (\tilde{\mathbf{G}}^{\perp})^{1/2}$.

IV. CALCULATIONS

Calculations on the $H + H_2 \rightarrow H_2 + H$ reaction have been carried out using the double many-body expansion (DMBE) potential of Varandas *et al.*[42] for the lowest electronically adiabatic state. For the reaction $O(^3P) + H_2 \rightarrow OH + H$, we employ the $^3A''$ potential of Joseph and two of the authors denoted $J3$[43] and for the reaction $CH_3 + H_2 \rightarrow CH_4 + H$, we use surface $J3$ of Joseph, Steckler, and one of the authors.[44]

The harmonic frequencies as a function of distance along the reaction path were computed as described elsewhere[20,26] and above.

In addition to the harmonic frequencies, we also present calculations of thermal rate constants for reactions (R1)–(R3) by improved canonical variational theory[20(d),25(b),26] (ICVT). Details of the methods used in the calculations of the rates are also provided elsewhere.[20,22,25,26,45] Vibrational energy levels for reactions (R1) and (R2) were computed using the Morse I approximation[18] for the stretch and the harmonic approximation for the bend. For reaction (R3), energy levels for bound vibrations are computed by the Morse approximation III.[25(a)] Rotational partition functions are computed for the triatomic reactions by the quantum mechanical rigid rotor approximation and for reaction (R3) by the classical approximation.

Quantum mechanical effects on the reaction coordinate motion are included by the small-curvature semiclassical adiabatic ground-state (SCSAG) tunneling method.[22,26]

Tunneling occurs through the vibrationally adiabatic ground-state potential energy curve given by

$$V_a^G(s) = V_{MEP}(s) + \epsilon_{int}^G(s), \qquad (117)$$

where $\epsilon_{int}^G(s)$ is the total vibrational zero-point energy summed over all vibrational modes. The contribution to $\epsilon_{int}^G(s)$ from modes with imaginary frequencies is taken as zero. In the SCSAG method, the effect of reaction path curvature is included by an effective mass for tunneling which is dependent on the reaction coordinate and contains contributions from all the vibrational modes treated in the independent-normal-mode approximation. Again we set contributions from modes with imaginary frequencies equal to zero. Combining the SCSAG transmission coefficient with ICVT rate constant yields the final (ICVT/SCSAG) rate constant.

Since the s values given in the figures discussed below depend on the value of μ in Eq. (1), we note that in all cases we set this equal to the reduced mass for relative translational motion of the reactants.

V. RESULTS

A. $H + H_2 \rightarrow H_2 + H$

The harmonic bending frequency for reaction (R1) as a function of the reaction coordinate s is presented in Fig. 3. Notice that the frequencies computed using the Cartesian-vibration a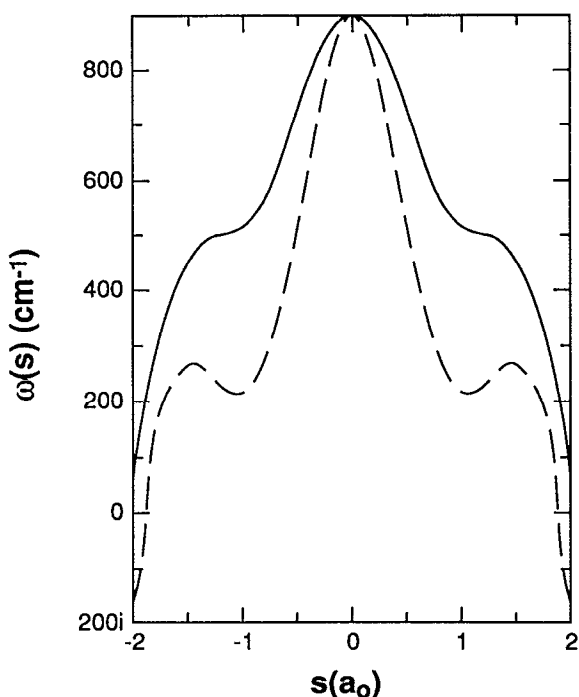nd bond-length reaction coordinates coincide at the saddle point ($s = 0$) as they must, but can be significantly different at other locations along the reaction path. For this reaction the potential is qualitatively well described by a London equation,[46] which predicts a tripletlike repulsion of the two end atoms. As pointed out in Sec. III, for this type of potential the bond-length reaction coordinate will give harmonic bending frequencies which are not imaginary. This is seen to be true for this case over a large region of the reaction path. The Cartesian-vibration bending frequency is seen to be always less than or equal to the bond-length frequency in this case.

Figure 4 shows the effect of the change in the harmonic bending frequency on the ground-state adiabatic potential curve. The lower adiabatic potential results from the drop in the bending frequency in going from the bond-length to the Cartesian-vibration reaction coordinate. The Cartesian-vibration reaction coordinate gives an adiabatic potential barrier that is thinner and will therefore give rise to enhanced tunneling.

Table I present the results of variational transition state theory (VTST) calculations of the rate constants for the two choices of reaction coordinate. In both cases, the improved canonical variational transition state occurs at the saddle point for all temperatures considered. Since the bending fre-
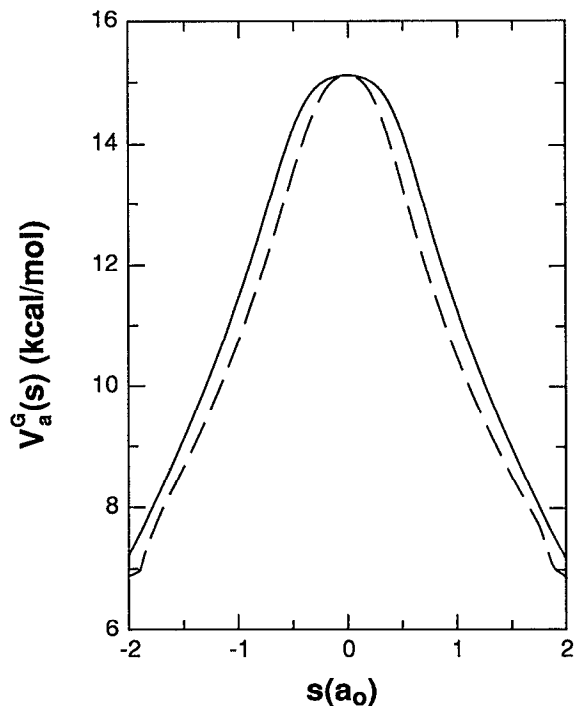

FIG. 3. Harmonic bending frequency for the $H + H_2$ reaction on the DMBE surface as a function of reaction coordinate s for two definitions of the reaction coordinate for bent geometries—the bond-length reaction coordinate (solid line) and the Cartesian-vibration reaction coordinate (dashed line). Frequencies plotted in the negative direction correspond to negative eigenvalues of the GF matrix and therefore imaginary frequencies. Plotting of sign$(\omega^2)|\omega|$ rather that ω^2 gives rise to discontinuities in the slopes of $\omega(s)$ when it passes through zero.

FIG. 4. Vibrationally adiabatic potential curve for the $H + H_2$ reaction on the DMBE surface as a function of reaction coordinate s for two definitions of the reaction coordinate for bent geometries—the bond-length reaction coordinate (solid line) and the Cartesian-vibration reaction coordinate (dashed line). For each choice of reaction coordinate the potential along the reaction path and the zero-point energy for the stretching vibration are identical; only the zero-point energy for the doubly-degenerate bending vibrations differs for the two curves. The zero-point energy levels are computed by the Morse I approximation for stretches and the harmonic approximation for bends.

TABLE I. Comparison of rate constants (units of cm^3 molecule^{-1} s^{-1}) for the reaction H + H$_2$ using the DMBE potential energy surface for computing the bending frequency in bond-length (BL) and Cartesian-vibration (CV) reaction coordinates.[a]

T,K	BL reaction coordinate		CV reaction coordinate	
	ICVT	ICVT/SCSAG	ICVT	ICVT/SCSAG
200	2.3×10^{-20}	1.1×10^{-18}	2.3×10^{-20}	5.7×10^{-18}
300	3.9×10^{-17}	1.9×10^{-16}	3.9×10^{-17}	4.6×10^{-16}
400	1.6×10^{-15}	3.7×10^{-15}	1.6×10^{-15}	6.5×10^{-15}
600	6.8×10^{-14}	9.8×10^{-14}	6.8×10^{-14}	1.3×10^{-13}
1000	1.7×10^{-12}	1.9×10^{-12}	1.7×10^{-12}	2.1×10^{-12}
1500	1.1×10^{-11}	1.1×10^{-11}	1.1×10^{-11}	1.2×10^{-11}
2400	5.8×10^{-11}	6.0×10^{-11}	5.9×10^{-11}	6.1×10^{-11}

[a] Rate constants are calculated using the Morse III approximation [Ref. 25(a)] for vibrational anharmonicity. For this case the Morse III approximation is the same as using Morse I for stretches and harmonic for bends.

quencies coincide there, the ICVT rate constants are identical for the two choices of reaction coordinate. However, when tunneling is included significant changes are seen. The thinner adiabatic barrier for the Cartesian-vibration reaction coordinate gives an enhancement of over a factor of 5 at 200 K. We know for H + H$_2$ though that calculations based on the bond-length reaction coordinate are in excellent agreement with accurate quantum mechanics when the anharmonicity is treated as accurately as possible for the stretch and bend and the same potential energy surface is used for both approximate and accurate calculations.[20(b),20(e),22]

Thus the use of the Cartesian-vibration reaction coordinate (or the least-squares coordinate system which gives the same frequencies) does not appear to be accurate in this case. We attribute this to neglect of bend–stretch interactions, which are expected, based on previous work[47,48] to be very important for Cartesian vibrations but relatively unimportant when bends are treated as occurring along curvilinear bend coordinates with fixed bond lengths. In particular, our previous experience with Cartesian and curvilinear vibrational coordinates for potential energy surfaces[47] and partition functions[48] of bound triatomics showed that when mode–mode coupling is neglected, as it is here and as it is often required in many other applications for practical reasons, the curvilinear bend coordinate leads to much better results than the Cartesian one.

B. O(^{3}P)+H$_2$ →OH+H

The trends for reaction (R2) are similar to those seen for the H + H$_2$ reaction. The potential used here for reaction (R2) describes the bend in terms of a purely repulsive anti-Morse function in the distance between the end atoms. As a result, the bending frequencies obtained using the bond-length reaction coordinate are real over the whole length of the reaction path shown in Fig. 5. In contrast, the frequencies obtained with the Cartesian-vibration reaction coordinate become imaginary very close to the saddle point: between $s = -0.14$ and $-0.16 a_0$ on the reactant side and between $s = 0.22$ and $0.24 a_0$ on the product side.

As for reaction (R1), the lower frequencies with the Cartesian-vibration reaction coordinate lead to a thinner

ground-state adiabatic barrier as seen in Fig. 6. The figure also shows that the adiabatic barrier for the bond-length reaction coordinate has a higher barrier which is shifted further towards reactants than the barrier for the Cartesian-vibration reaction coordinate; For the bond-length reaction coordinate, the maximum is 17.12 kcal/mol and it occurs at $s = -0.11 a_0$, whereas for the Cartesian-vibration reaction coordinate, the maximum is 16.89 kcal/mol and occurs at $s = -0.03 a_0$.

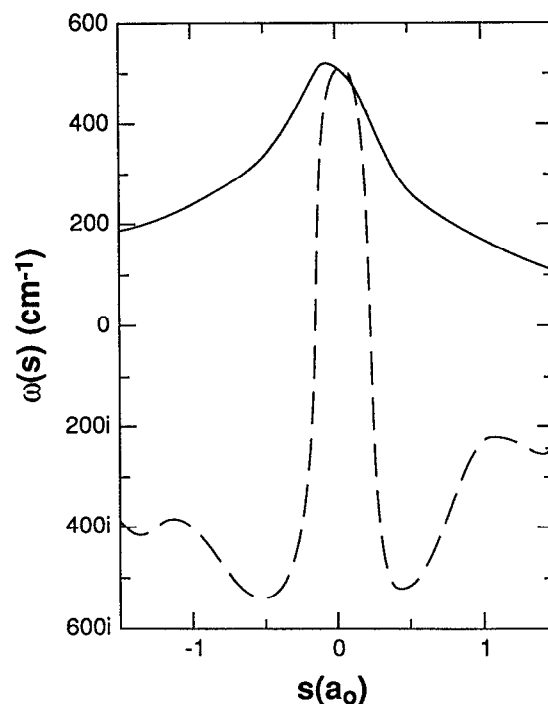As a result of the different maxima in the adiabatic barrier, even the ICVT rate constants (neglecting tunneling)

FIG. 5. Same as Fig. 1 except for the O + H$_2$ reaction on surface *J* 3 and, since some of these frequencies are imaginary, the quantity plotted is sign(ω^2)$|\omega|$. Thus, frequencies plotted in the negative direction correspond to negative eigenvalues of the GF matrix and are imaginary frequencies. Plotting of sign(ω^2)$|\omega|$ rather that ω^2 gives rise to discontinuities in the slopes of $\omega(s)$ when it passes through zero.
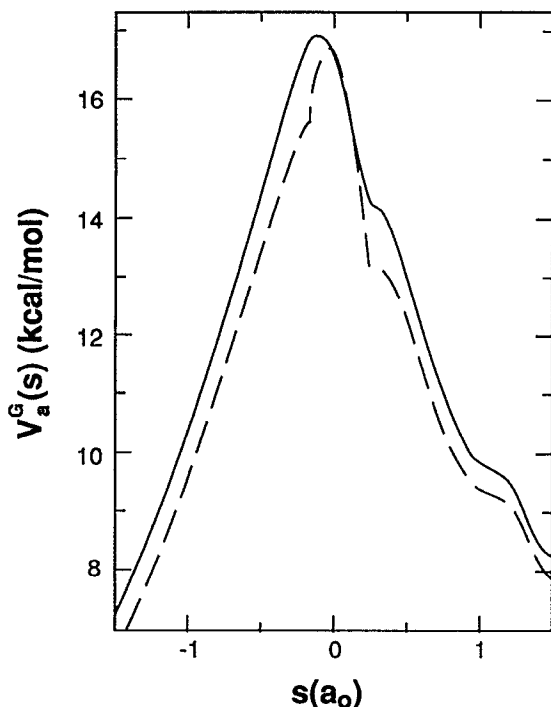
FIG. 6. Same as Fig. 2 except for the $O + H_2$ reaction on surface $J3$.

Cartesian-vibration reaction coordinate (or the least-squares coordinate system) is inaccurate when stretch–bend interactions are neglected.

One aspect of the $O + H_2$ results is very dramatic and deserves special comment. At every point on the collinear MEP, if we bend the system with fixed bond lengths the energy goes up. Nevertheless, Fig. 5 shows that the bend frequency computed with a Cartesian-vibration reaction coordinate may be imaginary. This is intuitively unphysical. A naive interpretation of imaginary-frequency vibrations along a reaction path is that the path has bifurcated. This temptation is especially tempting for polyatomic systems where the multidimensional geometry space is harder to describe in simple coordinates or to visualize. But the present example in which the collinear MEP clearly does not bifurcate, provides an easily visualized counterexample to the naive interpretation. A better way to "explain" the imaginary frequency is that the Cartesian vibrations, being "mathematical" and nonseparable, mix in some of the mode that "physically" corresponds to moving downhill along the path; thus, the energy goes down along this coordinate [see Eq. (14) for the way that this gradient along the MEP mixes into the vibrational force constants]. A curvilinear bend coordinate, such as the one used in defining the bond-length reaction coordinate, allows the system to bend without moving downhill on the MEP, i.e., it provides a more physical *separation* of the reaction coordinate from the bends.

C. $CH_3 + H_2 \rightarrow CH_4 + H$

Both reaction coordinates of Sec. III B (MEF–CV and BL) are defined the same way in the subspace of C_{3v} symmetries, and this algorithm is also identical to that used for the least-squares reaction coordinate of Ref. 23. Furthermore, as proved in Ref. 23, the use of the least-squares (LS) reaction coordinate for evaluating harmonic frequencies gives exactly the same results (not only for symmetry-breaking frequencies, but also for totally symmetric ones) as evaluating them by means of the Miller–Handy–Adams projection technique[21] involving Cartesian vibrations (CV). Thus, there are four approaches available and they all give the same frequencies for totally symmetric vibrations, but they give three different sets of frequencies for symmetry-break-

will differ for the two choice of reaction coordinate in this case. This is confirmed in Table II, which shows that using the bond-length reaction coordinate yields ICVT rate constants that are factors of 1.7 to 1.2 lower than those obtained using the Cartesian-vibration reaction coordinate over the temperature range from 200 to 2400 K. When tunneling is included in the ICVT/SCSAG rate constants, the difference becomes larger because the thinner barrier of the Cartesian-vibration reaction coordinate allows more tunneling. Thus, the differences of the ICVT/SCSAG rate constants using the Cartesian-vibration reaction coordinates from those calculated with the bond-length one are factors 7.4 to 1.3. Again the differences are large compared to the known[20(e),49] high accuracy attainable with the bond-length reaction coordinate for this reaction. We conclude that a treatment with the

TABLE II. Comparison of rate constants (units of cm^3 molecule^{-1} s^{-1}) for the reaction $O(^3P) + H_2$ using the $J3$ potential energy surface for computing the bending frequency in bond-length (BL) and Cartesian-vibration (CV) reaction coordinates.[a]

T,K	BL reaction coordinate		CV reaction coordinate	
	ICVT	ICVT/SCSAG	ICVT	ICVT/SCSAG
200	7.0×10^{-23}	1.9×10^{-20}	1.2×10^{-22}	1.4×10^{-19}
300	5.9×10^{-19}	7.3×10^{-18}	8.6×10^{-19}	2.8×10^{-17}
400	5.6×10^{-17}	2.3×10^{-16}	7.6×10^{-17}	6.1×10^{-16}
600	6.1×10^{-15}	1.1×10^{-14}	7.6×10^{-15}	2.0×10^{-14}
1000	3.3×10^{-13}	4.2×10^{-13}	4.0×10^{-13}	5.9×10^{-13}
1500	3.2×10^{-12}	3.6×10^{-12}	3.9×10^{-12}	4.6×10^{-12}
2400	2.4×10^{-11}	2.5×10^{-11}	3.0×10^{-11}	3.2×10^{-11}

[a] Rate constants are calculated using the Morse III approximation for vibrational anharmonicity.

ing vibrations. We have calculated all three sets, and we will label them CV, MEF–CV, and BL. In this section, we compare the results. First we compare the three sets of frequencies; then we compare rate constants calculated using the three sets of frequencies.

Of the four doubly-degenerate symmetry-breaking modes of the CH_5 complex, the frequencies of the two lowest-energy modes tend to zero in the asymptotic reactant region and the frequency of the lowest mode also tends to zero in the asymptotic product region. The lowest mode corresponds to a CHH' bend and thus its frequency tends to zero whenever the CH or HH' distance becomes infinite. The second lowest mode corresponds to the bending of the CH bond relative to the distance of C to the center-of-mass of the $H_a H_b H_c$ triangle (denoted a ΔCH bend) and therefore its frequency tends to zero only when the CH bond becomes infinite. The other two symmetry-breaking modes correspond to relative motions of the three H atoms in the triangle with respect to the C atom and therefore their frequencies tend to positive values in the asymptotic regions.

Figure 7 shows that the largest differences between frequencies for the symmetry-breaking modes computed using
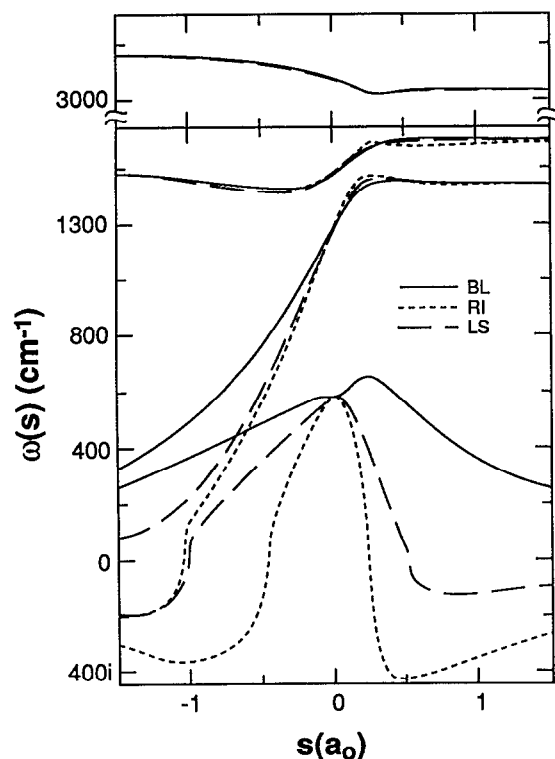
the different definitions of reaction coordinates occur for those modes whose frequencies are heading towards zero. Only very small changes in the frequencies are seen for the highest two symmetry-breaking modes and even for the second lowest mode in the product channel in which it tends to a positive-frequency motion. With the conventional, i.e., Cartesian-vibration reaction coordinate, the frequency becomes imaginary for the lowest mode between $s = -1.04$ and $-1.03\ a_0$ in the reactant channel and between $s = 0.50$ and $0.51\ a_0$ in the product channel. Going to the intermediate methyl-Eckart-frame Cartesian-vibration reaction coordinate, the situation becomes worse—the same frequency becomes imaginary at $s \cong -0.47\ a_0$ in the reactant channel at $s \cong 0.23\ a_0$ in the product channel. Although the lowest mode is the only one with imaginary frequencies for the Cartesian-vibration reaction coordinate, for the intermediate methyl-Eckart-frame Cartesian-vibration reaction coordinate, the second lowest frequency also becomes imaginary near $s \cong -1.06\ a_0$. For the bond-length reaction coordinate, all the frequencies remain real over the whole range of reaction coordinate that was studied ($s = -1.5$ to $1.5\ a_0$).

The vibrationally adiabatic ground-state potential curve shown in Fig. 8 reflects these differences in frequencies for the difference choices of reaction coordinate. As in the two triatomic reactions, the bond-length reaction coordinate gives the thickest adiabatic barrier and the largest maxi-
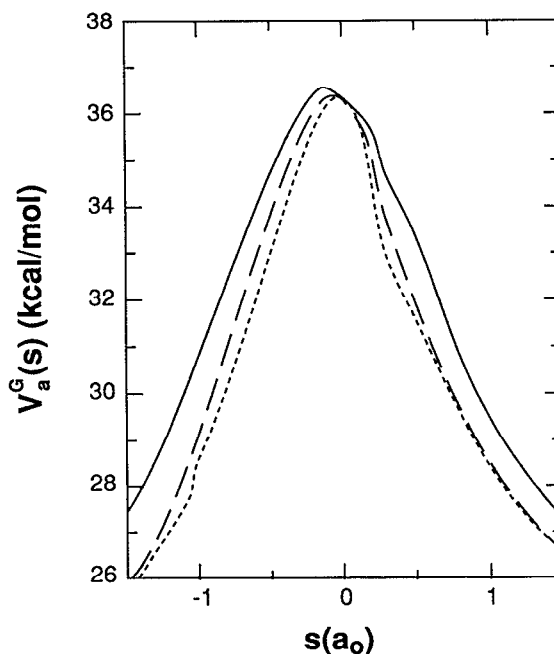

FIG. 7. Harmonic frequency (with the convention of Figs. 3 and 5 for imaginary frequencies) of the symmetry-breaking vibrations for the $CH_5 + H_2$ reaction on surface J 3 as a function of reaction coordinate s for three definitions of the reaction coordinate for nonsymmetric geometries—the bond length reaction coordinate (solid curves labeled BL), the methyl-Eckart-frame Cartesian-vibration reaction coordinate (short-dashed curves labeled RI), and the Cartesian-vibration reaction coordinate (long-dashed curves labeled LS). Four sets for frequencies are presented for the four doubly-degenerate symmetry-breaking modes. Note the break in the frequency scale at 1600 cm^{-1} which resumes at 2900 cm^{-1}.

FIG. 8. Vibrationally adiabatic potential curve for the $CH_3 + H_2$ reaction on surface J 3 as a function of reaction coordinate s for three definitions of the reaction coordinate for nonsymmetric geometries—the fixed-bond length reaction coordinate (solid curves), the MEF–CV reaction coordinate (short-dashed curves), and the CV (least-squares) reaction coordinate (long-dashed curves). For each choice of reaction coordinate the potential along the reaction path and the zero-point energy for the totally symmetric vibrations are identical; only the zero-point energy for the doubly-degenerate symmetry-breaking vibrations differ for the two curves. The zero-point energy levels are computed by the Morse III approximation.

TABLE III. Rate constants (cm^3 molecule^{-1} s^{-1}) for the reaction $CH_3 + H_2 \rightarrow CH_4 + H$ using the $J3$ potential energy surface with three methods to obtain the generalized-normal-mode vibrational frequencies.[a]

T(K)	CV		MEF–CV		BL	
	ICVT	ICVT/SCSAG	ICVT	ICVT/SCSAG	ICVT	ICVT/SCAG
200	9.2×10^{-25}	4.0×10^{-22}	1.1×10^{-24}	1.5×10^{-21}	6.1×10^{-25}	3.4×10^{-23}
300	1.3×10^{-20}	1.5×10^{-19}	1.4×10^{-20}	3.7×10^{-19}	1.0×10^{-20}	4.9×10^{-20}
400	1.5×10^{-18}	5.5×10^{-18}	1.6×10^{-18}	9.6×10^{-17}	1.2×10^{-18}	2.9×10^{-18}
600	1.7×10^{-16}	3.1×10^{-16}	1.8×10^{-16}	3.9×10^{-16}	1.6×10^{-16}	2.3×10^{-16}
1000	1.0×10^{-14}	1.2×10^{-14}	1.0×10^{-14}	1.3×10^{-14}	9.7×10^{-15}	1.1×10^{-14}
1500	1.1×10^{-13}	1.2×10^{-13}	b	b	9.9×10^{-14}	1.1×10^{-13}
2400	1.0×10^{-12}	1.0×10^{-12}	b	b	8.1×10^{-13}	8.3×10^{-13}

[a] Rate constants are calculated using the Morse III approximation for vibrational anharmonicity in all cases.
[b] Rate constants were not calculated for these temperatures because the ICVT bottleneck is calculated to be in the region where the lowest frequency is imaginary.

mum. This leads to the lowest rate constants. The rate constants displayed in Table III show differences of over an order of magnitude at 200 K when the values for various definitions of the reaction coordinate are compared. The differences become smaller at higher temperatures—a factor of 1.2 at 2400 K.

Since our potential surface calibration[44] for reaction (R3) was based on calculations employing the Cartesian-vibration reaction coordinate and since the rate constant at $T \cong 600$ K played an important role in the calibration, it is very significant that the calculated rate constant at 600 K is lowered by a factor of 0.7 when the bond-length reaction coordinate is used. The bond-length reaction coordinate is more realistic when mode–mode coupling is neglected (as it was in the previous work[44] and also here). A factor of 0.7 at 600 K is approximately equivalent to a 0.4 kcal/mol change in barrier height and it means that barrier heights inferred on the basis of comparing the previously calculated rate constants[44] to experiment may be about 0.4 kcal/mol too high. Thus, the effects discussed in this paper may be very significant for modeling efforts.

VI. SUMMARY AND CONCLUSIONS

We have shown that, even if the vibrational coordinates intersect the reaction path orthogonally, the harmonic reaction-path frequencies depend on the definition of the reaction coordinate s for configurations which do not lie on the MEP, but they are independent of the choice of the vibrational coordinates q for the given s.[23] The present paper illustrates this dependence for three reactions.

As a first example, we considered atom–diatom reactions with collinear minimum-energy paths and we showed how two different definitions of the reaction coordinate for nonlinear geometries give different bend frequencies. The two reaction coordinates considered are the Cartesian-vibration reaction coordinate (which for these reactions yields results equivalent to using either of two formalisms presented previously, namely the Miller–Handy–Adams projection technique[21,26] or the "least-squares" reaction coordinate[23]) and the bond-length reaction coordinate, which has also been used previously.[20] We also show that the use of the bond-length reaction coordinate will always give real values for the bending frequency when the fixed-bond-lengths bend potential is purely repulsive. As an illustration, this analysis was applied to the reactions $H + H_2$ and $O + H_2$.

As a final example we considered the reaction $CH_3 + H_2$ using two new coordinate systems for $CX_3 YZ$ presented here. In one new coordinate system for reaction path dynamics of the polyatomic reaction $CX_3 + YZ \rightarrow CX_3 Y + Z$, the reaction coordinate is assumed constant using curvilinear vibrational coordinates corresponding to $CX_3 Y$ deformations with fixed bond lengths. For $CX_3 + YZ$ reactions, both new reaction coordinates lead to different results than the conventional Cartesian-vibration treatment.

The results of this article show that there is significant difference between the harmonic frequencies along the reaction path when different reaction coordinates are used. Thus, the conceptually appealing model of dynamics based on a harmonic reaction-path potential, which is very convenient for many purposes, should always be interpreted with a cautious regard for the nonuniqueness of the harmonic Hamiltonian and a consideration of whether this affects the dynamical conclusions. As one striking example, we have shown that an imaginary generalized normal mode frequency does not necessarily signal a bifurcation of the reaction path. In the case treated here, the reaction coordinates defined in terms of bond lengths give the most physical results. Further exploration of the effect of reaction coordinate choice on harmonic reaction path potentials, as well as the treatment of anharmonicity and vibration–rotation coupling, would be very interesting.

ACKNOWLEDGMENTS

[1] I. Shavitt, University of Wisconsin Theoretical Chemistry Laboratory Technical Report No. WIS-AEC-23 (Madison, Wisconsin, 1959); I. Shavitt, J. Chem. Phys. **49**, 4048 (1968).

[2] G. L. Hofacker, Z. Naturforsch. Teil A **18**, 607 (1963).

[3] H. S. Johnston and C. A. Parr, J. Am. Chem. Soc. **85**, 2544 (1963); H. S. Johnston, *Gas Phase Reaction Rate Theory* (Ronald, New York, 1966).

[4] R. A. Marcus, J. Chem. Phys. **41**, 610 (1964); R. A. Marcus, J. Chem. Phys. **45**, 4493, 4500 (1966).

[5] R. A. Marcus, J. Chem. Phys. **49**, 2610 (1968).

[6] R. A. Marcus, J. Chem. Phys. **49**, 2617 (1968); **53**, 4026 (1970); R. A. Marcus and M. E. Coltrin, J. Chem. Phys. **67**, 2609 (1977).

[7] M. S. Child, Discuss. Faraday Soc. **44**, 68 (1968).

[8] R. E. Wyatt, J. Chem. Phys. **51**, 3489 (1969); M. J. Redmon and R. E. Wyatt, Int. J. Quantum Chem. Symp. **9**, 403 (1975); **11**, 343 (1977).

[9] D. G. Truhlar, J. Chem. Phys. **53**, 2041 (1970); D. G. Truhlar and A. Kuppermann, J. Am. Chem. Soc. **93**, 1840 (1971); Chem. Phys. Lett. **9**, 299 (1971); B. C. Garrett and D. G. Truhlar, J. Phys. Chem. **83**, 200, 3058 E (1979).

[10] J. C. Light, Adv. Chem. Phys. **19**, 1 (1971).

[11] G. L. Hofacker and R. D. Levine, Chem. Phys. Lett. **9**, 517 (1971); R. D. Levine, Chem. Phys. Lett. **10**, 510 (1971); G. L. Hofacker and R. D. Levine, Chem. Phys. Lett. **15**, 165 (1972); A. Ben-Shaul and G. L. Hofacker, in *Handbook of Chemical Lasers*, edited by R. W. F. Gross and J. F. Bott (Wiley, New York, 1976), p. 579.

[12] S. F. Fischer and M. A. Ratner, J. Chem. Phys. **57**, 2769 (1972).

[13] K. Fukui, in *The World of Quantum Chemistry*, edited by R. Daudel and B. Pullman (Reidel, Dordrecht, Holland, 1974), p. 113; K. Fukui, S. Kato, and H. Fujimoto, J. Am. Chem. Soc. **97**, 1 (1975); K. Ishida, K. Morokuma, and A. Komornicki, J. Chem. Phys. **66**, 2153 (1977); S. Kato and K. Morokuma, J. Chem. Phys. **73**, 3900 (1980); K. Fukui, Acc. Chem. Res. **14**, 363 (1981); K. Morokuma and S. Kato, in *Potential Energy Surfaces and Dynamics Calculations*, edited by D. G. Truhlar (Plenum, New York, 1981), p. 243; K. Morokuma, S. Kato, K. Kitaura, S. Obara, K. Ohta, and M. Hanamura, in *New Horizons of Quantum Chemistry*, edited by P.-O. Löwdin and B. Pullman (Reidel, Dordrecht, Holland, 1983), p. 221.

[14] J. W. Duff and D. G. Truhlar, J. Chem. Phys. **62**, 2477 (1975); D. G. Truhlar and D. A. Dixon, in *Atom–Molecule Collision Theory*, edited by R. D. Bernstein (Plenum, New York, 1979), p. 595.

[15] H. F. Schaefer III, Chem. Brit. **11**, 227 (1975); W. H. Miller, Y. Yamaguchi, and H. F. Schaefer III, J. Chem. Phys. **73**, 2733 (1980).

[16] (a) M. V. Basilevsky, Chem. Phys. **24**, 81 (1977); (b) M. V. Basilevsky, J. Mol. Struct. **103**, 139 (1983).

[17] M. V. Basilevsky and V. M. Ryaboy, Chem. Phys. **41**, 461, 477 (1979).

[18] B. C. Garrett and D. G. Truhlar, J. Phys. Chem. **83**, 1052, 1079 (1979); D. G. Truhlar and B. C. Garrett, Acc. Chem. Res. **13**, 440 (1980); B. C. Garrett, D. G. Truhlar, and R. S. Grev, in *Potential Energy Surfaces and Dynamics Calculations*, edited by D. G. Truhlar (Plenum, New York, 1981), p. 587.

[19] B. C. Garrett and D. G. Truhlar, J. Chem. Phys. **70**, 1593 (1979).

[20] (a) B. C. Garrett and D. G. Truhlar, J. Am. Chem. Soc. **101**, 4534 (1979); (b) B. C. Garrett and D. G. Truhlar, Proc. Natl. Acad. Sci. USA **76**, 4755 (1979); (c) B. C. Garrett and D. G. Truhlar, J. Chem. Phys. **72**, 3460 (1980); (d) B. C. Garrett, D. G. Truhlar, R. S. Grev, and A. W. Magnuson, J. Phys. Chem. **84**, 1730 (1980); **87**, 4554 E (1983); (e) B. C. Garrett, D. G. Truhlar, and G. C. Schatz, J. Am. Chem. Soc. **108**, 2876 (1986).

[21] W. H. Miller, N. C. Handy, and J. E. Adams, J. Chem. Phys. **72**, 99 (1980); W. H. Miller, in *Potential Energy Surfaces and Dynamics Calculations*, edited by D. G. Truhlar (Plenum, New York, 1981), p. 265; K. Yamashita and W. H. Miller, J. Chem. Phys. **82**, 5475 (1985); W. H. Miller, NATO ASI Ser. C **170**, 27 (1986).

[22] R. T. Skodje, D. G. Truhlar, and B. C. Garrett, J. Phys. Chem. **85**, 3019 (1981); D. G. Truhlar, A. D. Isaacson, R. T. Skodje, and B. C. Garrett, J. Phys. Chem. **86**, 2252 (1982); **87**, 4554 E (1983).

[23] G. A. Natanson, Mol. Phys. **46**, 481 (1982).

[24] R. T. Skodje, D. G. Truhlar, and B. C. Garrett, J. Chem. Phys. **77**, 5955 (1983); B. C. Garrett and D. G. Truhlar, J. Chem. Phys. **79**, 4931 (1983); R. T. Skodje, D. W. Schwenke, D. G. Truhlar, and B. C. Garrett, J. Phys. Chem. **88**, 628 (1984).

[25] (a) A. D. Isaacson and D. G. Truhlar, J. Chem. Phys. **76**, 1380 (1982); (b) S. N. Rai and D. G. Truhlar, J. Chem. Phys. **79**, 604 (1983); (c) F. B. Brown, S. C. Tucker, and D. G. Truhlar, J. Chem. Phys. **83**, 4451 (1985).

[26] D. G. Truhlar, A. D. Isaacson, and B. C. Garrett, in *Theory of Chemical Reaction Dynamics*, edited by M. Baer (CRC, Boca Raton, FL, 1985), Vol. 4, p. 65.

[27] A. Tachibana, I. Okazaki, M. Koizumi, K. Hori, and T. Yamabe, J. Am. Chem. Soc. **107**, 1190 (1985); A. Tachibana, H. Fueno, and T. Yamabe, J. Am. Chem. Soc. **108**, 4346 (1986).

[28] M. A. Schmidt, M. S. Gordon, and M. Dupuis, J. Am. Chem. Soc. **107**, 2585 (1985); B. C. Garrett, M. J. Redmon, R. Steckler, D. G. Truhlar, K. K. Baldridge, D. Bartol, M. W. Schmidt, and M. S. Gordon, J. Phys. Chem. **92**, 1476 (1988); D. G. Truhlar and M. S. Gordon, Science **249**, 491 (1990).

[29] D. G. Truhlar, F. B. Brown, R. Steckler, and A. D. Isaacson, NATO ASI Ser. C **170**, 285 (1986); A. D. Isaacson, D. G. Truhlar, S. N. Rai, R. Steckler, G. C. Hancock, B. C. Garrett, and M. J. Redmon, Comput. Phys. Commun. **47**, 91 (1987); G. C. Hancock and D. G. Truhlar, J. Chem. Phys. **90**, 3498 (1989).

[30] T. H. Dunning, Jr., E. Kraka, and R. A. Eades, Faraday Discuss. Chem. Soc. **84**, 427 (1987).

[31] C. Doubleday, Jr., M. Page, and J. W. McIver, Jr., J. Mol. Struct. (Theochem.) **163**, 331 (1988); M. Page and J. W. McIver, Jr., J. Chem. Phys. **88**, 922 (1988); C. Doubleday, Jr., J. W. McIver, Jr., and M. Page, J. Phys. Chem. **92**, 4367 (1988); M. Page, J. Phys. Chem. **93**, 3639 (1989); M. Page, M. C. Lin, Y. He, and T. K. Choudhury, J. Phys. Chem. **93**, 4404 (1989); M. Page, C. Doubleday, and J. W. McIver, Jr., J. Chem. Phys. **93**, 5634 (1990).

[32] N. Shida, J. E. Almlöf, and P. F. Barbara, Theor. Chim. Acta. **76**, 7 (1989); N. Shida, P. F. Barbara, and J. E. Almlöf, J. Chem. Phys. **91**, 4061 (1989).

[33] N. R. Walet, A. Klein, and G. D. Dong, J. Chem. Phys. **91**, 2848 (1989).

[34] G. A. Natanson, J. Chem. Phys. **93**, 6589 (1990).

[35] E. B. Wilson, Jr., J. C. Decius, and P. C. Cross, *Molecular Vibrations* (McGraw-Hill, New York, 1955).

[36] C. Eckart, Phys. Rev. **47**, 552 (1935).

[37] A. Sayvetz, J. Chem. Phys. **7**, 383 (1939).

[38] G. A. Natanson, Chem. Phys. Lett. **134**, 301 (1987).

[39] G. A. Natanson, Chem. Phys. Lett. **149**, 551 (1988).

[40] R. Wallace, Chem. Phys. **88**, 247 (1984).

[41] C. F. Curtiss, J. O. Hirschfelder, and F. T. Adler, J. Chem. Phys. **18**, 1638 (1950).

[42] A. J. C. Varandas, F. B. Brown, C. A. Mead, D. G. Truhlar, and N. C. Blais, J. Chem. Phys. **86**, 6258 (1987).

[43] T. Joseph, D. G. Truhlar, and B. C. Garrett, J. Chem. Phys. **88**, 6982 (1988).

[44] T. Joseph, R. Steckler, and D. G. Truhlar, J. Chem. Phys. **87**, 7036 (1987).

[45] A. D. Isaacson, D. G. Truhlar, S. N. Rai, R. Steckler, G. C. Hancock, J. G. Lauderdale, T. N. Truong, T. Joseph, B. C. Garrett, and R. Steckler, POLYRATE Program Manual, Version 1.5, University of Minnesota Supercomputer Institute Research UMSI 88/87 (1988).

[46] F. London, Z. Elektrochem. **35**, 552 (1929).

[47] M. A. Pariseau, I. Suzuki, and J. Overend, J. Chem. Phys. **42**, 2335 (1965).

[48] A. D. Isaacson, D. G. Truhlar, K. Scanlon, and J. Overend, J. Chem. Phys. **75**, 3017 (1981).

[49] K. Haug, D. W. Schwenke, D. G. Truhlar, Y. Zhang, J. Z. H. Zhang, and D. J. Kouri, J. Chem. Phys. **87**, 1892 (1987); J. Z. H. Zhang, Y. Zhang, D. J. Kouri, B. C. Garrett, K. Haug, D. W. Schwenke, and D. G. Truhlar, Faraday Discuss. Chem. Soc. **84**, 371 (1987).